NORTH-WEST UNIVERSITY
YUNIBESITI YA BOKONE-BOPHIRIMA
NOORDWES-UNIVERSITEIT

Synthesis and Characterisation of TiO_2 (titanium dioxide) nanomaterials and Au / TiO_2 (gold titanium dioxide) nanocomposites

By

Kelebile Pearl Maizie Seoposengwe (16774809)

B.Sc. Honours Chemistry (North-West University, South Africa)

A thesis submitted in fulfilment of the requirements for the Master's degree in Chemistry

In the Faculty of Agriculture, Science and Technology

(Department of Chemistry)

North-West University : Mafikeng Campus

Supervisor: Dr Mbhuti Hlophe

Co-supervisor: Dr Lucky Sikhwivhilu

2012

DECLARATION

I Kelebile Pearl Maizie Seoposengwe declare that this project which is submitted in fulfillment of the requirements for the degree of Master of Science in Chemistry (M.Sc.) at North West University, Mafikeng Campus has not been previously submitted for a degree at this university or any other university. The following research was compiled, collated and written by me. All the quotations are indicated by appropriate punctuation marks. Sources of my information are acknowledged in the reference pages.

....

Kelebile Pearl Maizie Seoposengwe Date

ACKNOWLEDGEMENTS

I would like to express my sincere gratitude to Dr M.R Hlophe, my supervisor for his valuable insights and inspiration in this project.

I would also like to thank my co–supervisor Dr L.M. Sikhwivhilu for his guidance and support throughout this journey as well as Prof. Selvaratnam and the Chemistry department for their support.

I also wish to thank the following people: My grandmother and family for praying for me, my aunt Mrs R. Shongwe and her husband for taking care of me since my parents passed away, my colleague and friend, Miss L. Metswamere for her assistance and support, chemistry technicians, Mr Murulana and Mr Peter Mahlangu, Miss Z. Milongo, Miss G. Kanyane, Miss L. Mpofu and Mr M. Ndaba, my siblings (Ontisitse, Keabetswe and Kgomotso) and all my friends

May God bless you all

I would really like to dedicate this research project to my late parents, Mr and Mrs Seoposengwe, and my grandfather. May God bless their beautiful souls.

I would also like to thank myself for all the hard-work and perseverance

NWU Masters for funding, CSIR building 19 a and b for letting me use their equipments for my practical.

And finally I would like to thank God almighty for giving me the strength, patience and perseverance to complete this project.

ABSTRACT

The Au / TiO_2 nanocomposites were synthesized by the incipient wetness impregnation method. The TiO_2 supports were first prepared and then Au was loaded on them. The TiO_2 nanomaterials were synthesized by the hydrothermal method, using TiO_2 (P-25 Degussa) containing 80 % anatase and 20 % rutile and NaOH, NH_4OH, and KOH. TiO_2 was treated with 18 M NaOH and then NH_4OH was introduced as co –solvent, using different volumes. The materials were then characterized by SEM, TEM, XRD, BET, EDX and FTIR, to determine morphology and structure. 18 M NaOH concentration did not transform the spherical morphology of TiO_2 but there was structural transformation. The samples treated with NH_4OH were also found to be spherical in shape, but they were composed of clustered aggregates. NH_4OH did not influence the morphology and the structure of the material, since it is considered to be a weak base.

Then KOH and NaOH were used with three different mole ratios to check the influence of these bases on the structural and morphological transformation of the material. It was observed that the morphology transformation was dependent on the amount of KOH that was added. The morphology transformation decreased with a decrease in the amount of KOH. A mixture of nanotubes and nanorods were obtained, with average diameters of 4-11 nm and 3-18 nm for samples B1 and B2 respectively. The variation in the amount of KOH resulted in nanobelts and nanorods.

The samples were then calcined at 300 °C. It was found that the calcination temperature did not affect the crystallinity but it affected the morphology because no unreacted material was observed.

Then the loading of Au followed. Incipient wetness impregnation was used. Samples B1 and B2 and TiO_2 P-25 Degussa were used as supports for Au particles, and they were later re-named samples C2, C3 and C1 respectively. $HAuCl_4.3H_2O$ was used as the source of Au. The TEM results showed the presence of Au particles. The Au particles were found to be well dispersed on the spherical morphology than on the tubular morphology. EDX also confirmed the presence of Au on the materials. The surface areas of samples C2 and C3 increased due to the structural transformation.

TABLE OF CONTENTS

CHAPTER 3

CHAPTER 4

Hydrothermal processing of TiO_2 nanostructures: The effect of NaOH / NH_4OH ratio on TiO_2 nanostructures

CHAPTER 5

Hydrothermal processing of TiO_2 nanostructures :The effect of KOH/ NaOH mole ratio on the TiO_2 nanostructures

CHAPTER 6

The effect of calcination on the TiO_2 nanomaterials treated with NH_4OH/ NaOH solutions.

CHAPTER 7

The effect of calcination on the TiO_2 nanomaterials (KOH/ NaOH mole ratio)

CHAPTER 8

The effect of loading Au on the TiO_2 nanomaterials

CHAPTER 9

LIST OF TABLES

LIST OF FIGURES

Definition of concepts and abbreviations

CONCEPTS

Doping- is a process of intentionally introducing impurities into an extremely pure semiconductor to change its properties.

Nanoparticles- ultrafine particles sized between 1 and 100 nm.

Nanocomposite- Multiphase solid material where one of the phases has one, two or three dimensions of less than 100 nm.

Band gap- The term "band gap" refers to the energy difference between the top of the valence band and the bottom of the conduction band; electrons are able to jump from one band to another.

Plasmon absorption band- range of wavelengths, equivalently, in the electromagnetic spectrum which is able to excite a particular transition in a substance.

Calcination- is a thermal treatment process applied to ores and other solid materials in order to bring about thermal decomposition, phase transition, or removal of a volatile fraction.

Desiccator - is a sealable enclosures containing dessicants that are used for preserving moisture sensitive reagents or chemicals

Deionised water - is the water from any source that is physically processed to remove impurities

Mesoporous material - it is a material that contains pores with diameters between 2 and 50 nm.

Precursor – a compound that participates in the chemical reaction that is transformed into another.

Catalyst – a substance that accelerates a chemical reaction without itself being affected.

In situ expresses that the object has not been "newly" moved.

LIST OF ABBREVIATIONS

SEM- Scanning electron microscopy

TEM- Transmission electron microscopy

XRD- X-ray diffraction

FTIR – Fourier transform infrared spectroscopy

UV – VIS- ultra violet visible spectroscopy

HRTEM – High resolution transmission electron microscopy

$HAuCl_4$ – Chloroauric acid

KOH – Potassium hydroxide

NaOH – Sodium hydroxide

NH_4OH – Ammonium hydroxide

TiO_2 – Titanium dioxide or titania

Au – Gold

Au / TiO_2 – Gold titanium dioxide

BET – Brunauer – Emmett – Teller method

EDX- Energy dispersive x- ray spectroscopy

EtOH – Ethanol

CHAPTER 1

1.1 BACKGROUND

Nanoscience is the study of materials on the nanoscale level between approximately 1 and 100 nm, and it helps in controlling the formation of 2- and 3- dimensional assemblies of molecular-scale building blocks into well defined nanostructures or nanomaterials. At the nanoscale, properties of matter are novel and they exhibit astonishing biological, chemical and physical properties as compared to those observed at the microscale [1]. Nanotechnology is the manipulation of matter at the nanoscale. It can provide exceptional understanding about materials and devices and is likely to impact many fields of research. Nanotechnology is commonly considered as a general- purpose technology and has become a common technology for almost all technology sectors because of its ability to create super-functional properties at the nanoscale. It is a promising technology which is multidisciplinary in various fields such as physics, chemistry, materials sciences and biology. This technology was predicted by Richard Feynman, when he was addressing the American Physical Society in 1959 [2]. Feynman said that there is plenty of room at the bottom, which means that by reducing bulk matter to atomic scale there is an increase in surface area and that results in enhanced properties. And this implies that matter can be controlled and manipulated at a smaller scale. The important nano- objects include quantum dots and nanocrystals of metals, semiconductors, oxides and other materials as well as one-dimensional nanostructures such as nanotubes, nanospheres, nanorods and nanowires.

Nanotechnology has grown rapidly that it spurred a major importance in the environmental applications of nanomaterials. Due to their large specific surface area, nanomaterials are excellent adsorbents, catalysts and sensors. Nanomaterials possess novel properties that can be used in the development of new technologies and in the improvement of existing ones, owing to their size. These novel properties such as large surface area, potential for self assembly, high specificity, high reactivity and catalytic potential, makes them excellent candidates for the removal of contaminants in water. Several nanomaterials have shown to have strong antimicrobial properties. They have been shown to have the potential to replace or improve conventional disinfection methods if they are appropriately incorporated into treatment processes. Recently, nanoscience has been applied in electronics, catalysis and biomedical research. Nanotechnology is a promising field that is attracting general attention

in the international scientific community. Although there has been an extensive application of this technology in different areas such as medicine, pharmaceuticals, biotechnology and electronics, its application in the treatment of drinking water has been limited and it has been only recently that it has picked up [3].

TiO_2 nanomaterials are known to have novel properties, and they have been applied in sunscreens because they are able to absorb Ultraviolet light, and they have also been used in optical devices, coatings, paints, toothpaste and cosmetics. These nanomaterials have high photosensitivity and because of that they have been regarded as photocatalyst in the treatment of air and water, since they are known to be non-toxic and chemically inert. When TiO_2 is irradiated with Ultraviolet light, it works wonders in the degradation of organic pollutants. But because of its wide band-gap (E_g = 3.2 eV), it cannot absorb Ultraviolet light effectively. And this can be solved by loading and doping with other metal oxides and metals [4]. Several metals such as Au, Ag, Pt and Pd are the most common ones. TiO_2 that is either loaded or doped with Au have unique and improved properties. Au nanoparticles have been of great interest in both the industrial and environmental applications. TiO_2 has been regarded as the best support for Au. Au / TiO_2 nanocomposites have been synthesized for different uses such as carbon monoxide oxidation and this helps in environmental remediation, they have also been used in chemical industries and in commercial applications for the removal of offensive odour. Many methods have been employed in the synthesis of Au / TiO_2 nanocomposites, and they include incipient wetness- impregnation, deposition-precipitation, sol-gel, gas-phase grafting etc.

Not only are scientists and technology developers fascinated by the interesting opportunities of this emerging field, but policy makers also believe that nanotechnology is one of the key technologies of the 21st century that will create new markets and consequently prosperity [5,6,7,8,9]. In this study Au / TiO_2 nanocomposites were synthesized using the incipient wetness impregnation method.

1.2 Introduction

Titanium dioxide (TiO_2) is the most popular semiconductor metal–oxide with novel properties. It is chemically stable, cheap and non-toxic and because of its non-toxicity, it has been used in the environmental applications. It is an excellent support material for some metals, such as Au and Ag and Pd. However, it has a wide band- gap and that leads to some limitations for some applications. It is well known that the loading of some noble metals such as Au can enhance the properties of titania. TiO_2 P-25 Degussa is available commercially and it usually consists of 80 % anatase and 20 % rutile, and it has a surface area of 49 m^2 / g [9,10,11].

Naturally Au is inert in bulk form but when it is at the nanoscale it becomes catalytically active. Au nanoparticles have attracted much interest in both industrial and environmental applications. The activity of these nanoparticles is greatly influenced by the support on which they are deposited.

There are many methods employed in the synthesis of Au / TiO_2 and they include incipient-wetness impregnation, deposition-precipitation and co–precipitation. In the preparation of Au / TiO_2 nanocomposites, TiO_2 which is the support is usually prepared first and the loading follows later. For the preparation of TiO_2 support, there are many methods that can be employed such as sol–gel, microemulsion and hydrothermal method. Sol-gel leads to the amorphous phase, which then needs to be calcined at higher temperatures to make it crystalline, but that can lead to agglomeration and reduced surface area. Microemulsion is expensive and it leads to very low titania yield. However hydrothermal technique is rapid, convenient and cheap [9,11,12].

Hydrothermal method is known to produce titania nanomaterials using some bases such as KOH, NaOH and NH_4OH. Various morphologies such as nanotubes, nanowires, nanobelts, nanorods and nanospheres have been obtained by following this route [13].

1.3 Problem statement

Many communities lack adequate sanitation services especially the people from the rural areas who are still depending on rivers and lakes for their water supply. Water needs to be treated for the removal of pollutants. The conventional disinfection methods are chlorination, chloroamination, uv – disinfection, and ozonation. Chlorination is effective for the removal of pathogenic microbes. The drawback of this method is that chlorine can react with naturally occurring organic compounds in the water supply to produce disinfection BY-PRODUCTS (DBPs) which are carcinogenic. Chloroamination provides longer lasting water treatment but its disadvantage is that it also reacts with organics to form DBPs. The disadvantage of UV-disinfection is that unlike chlorination it leaves no residual disinfectant in water. Ozonation is an effective method to inactivate harmful protozoa and other pathogens. However, it also forms toxic by- products in water.

TiO_2 is a well known semiconductor photocatalyst and is known to degrade organics and inactivate pathogenic microbes. Since titania is non-toxic, its photocatalytic properties have been utilized in various environmental applications to remove contaminants from both water and air for health protection. The antibacterial activity of TiO_2 is related to the production of reactive oxygen species (ROS). TiO_2 has a large band gap of 3.2 eV which is too wide to absorb visible light efficiently and that leads to some major limitations for its applications. Nano Au has novel properties and enhances the photocatalytic activity of a metal oxide support such as TiO_2 . Au / TiO_2 nanocomposites are used as active catalysts for the catalytic degradation of organic compounds and pathogenic microbes. Owing to the risks associated with the use of conventional disinfection technologies, the current project will investigate an optimum method for the synthesis of Au / TiO_2 nanocomposites that will be used for water disinfection.

1.4 Objectives

(a) To synthesize TiO_2 nanomaterials using various bases (NaOH, KOH, NH_4OH) and to characterize the obtained materials

(b) To check the influence of the base on the morphology transformation

(c) To load Au on the TiO_2 and to characterize Au / TiO_2 nanocomposites that are obtained

(d) To check the effect of loading Au on the TiO_2 support

1.5 References

1. Ju-Nam, Y. and Lead, J.R. (2008). **Manufactured nanoparticles : An overview of their chemistry, interactions and potential environmental implications**. Science of the Total Environment, **400** (1-3), 396-414.
2. Feynman, R.P. (1992). **There's Plenty of Room at the Bottom.** Journal of Microelectromechanical Systems, **1**(1), 60 - 67.
3. Kumar, R. (2011). **Development and Potential Applications of Nanomaterials for Arsenic Removal from contaminated Ground water.** TRITA LWR Degree project 11:07; 17p.
4. Belova, V., Borodina, T., Möhwald, H. and Shchukin, D.G.(2011). **The effect of high intensity ultrasound on the loading of Au nanoparticles into titanium dioxide.** Ultrasonics Sonochemistry, **18** (3), 310 – 317.
5. Islam, N. and Miyazaki, K. (2009). **Nanotechnology innovation system: Understanding hidden dynamics of nanoscience fusion trajectories.** Technological Forecasting and Social Change, **76** (1), 128-140.
6. Rao, C.N.R., Govindaraj, A., Gundiah,G. and Vivekchanol, S.R.C. (2004). **Nanotubes and nanowires.** Chemical Engineering Science, **59** (22-33), 4665-4671.
7. Suh, W.H., Suslick,K.S., Stucky,G.D. and Suh, Y.(2009). **Nanotechnology, nanotoxicology and neuroscience.** Progress in Neurobiology, **87** (3), 133-170.
8. Li, Q., Mahendra, S., Lyon, D.Y., Brunet, L., Liga, M.V., Li, D., and Alvarez, P.J.J. (2008). **Antimicrobial nanomaterials for water disinfection and microbial control: Potential applications and implications.** Water Research, **42** , 4591-4602.
9. Guan, J. and Ma, N. (2007). **China 's emerging presence in nanoscience and nanotechnology : A comparative bibliometric study of several nanoscience " giants".** Research Policy, **36** (6), 880-886.
10. Bacsa, R.R. and Kiwi, J. (1998). **Effect of rutile phase on the photocatalytic properties of nanocrystalline titania during the degradation of þ-coumaric acid.** Applied Catalysis B: Environmental, **16**, 19-29.
11. Primo, A., Corma, A., and Garcia, H. (2010). **Titania supported gold nanoparticles as photocatalyst**. Institution de Tecnologia Quimica , Universidad Politecnica de Valencia-CSIC, Camino de Vera,46022 Valencia, Spain.

12. Haruta M. (1997). **Size- and support- dependency in the catalysis of gold.** Catalysis Today, **36**, 153- 166.

13. Sikhwivhilu, L.M, Sinha Ray, S, and Coville, N.J.,(2009).**Influence of bases on hydrothermal synthesis of titanate nanostructures**. Applied Physics A Materials Science and Processing, **94**, 963-973.

CHAPTER 2

Literature survey

2.1 Significance of TiO_2 and Au

2.1.1 TiO_2

TiO_2 which is known as titania or titanium dioxide is a widely studied photocatalyst because of its outstanding properties which include strong oxidizing power and excellent chemical inertness. Titanium dioxide is the most stable semiconductor photocatalyst, it is available, affordable and non-toxic. For a solid to be a photocatalyst it must be stable and durable under irradiation [2]. And because of titania's non-toxicity it has been used for environmental remediation such as air and water purification. In cosmetic industries it has been used in toothpastes and sunscreens due to its ability to absorb ultraviolet light. It has a wide band-gap but it is too wide to absorb visible light efficiently. In order to overcome the problem of photoresponse of TiO_2 to visible light and to enhance the photocatalytic activity, doping or loading with noble metals or transition metals can be performed. TiO_2 exists in 3 crystalline phases : anatase which is metastable but the most active; rutile which is stable; brookite which is photocatalytically inactive. Various methods have been employed in the synthesis of TiO_2 nanoparticles and these include: the sulphate process, the chloride process, impregnation, co-precipitation, hydrothermal method, direct oxidation of $TiCl_4$, the metal organic chemical vapor deposition method and the sol- gel method. The sol gel method is the most popular method but its disadvantage is that it leads to an amorphous phase which can be made crystalline by calcination at moderate temperatures and that leads to a reduced surface area and agglomeration of particles. The photocatalytic activity is greatly influenced by the crystal structure, the size of the crystalline particles and the surface area. [1,2]

2.1.2 Au nanoparticles

Naturally Au in bulk form is the least active of the platinum group metals and it has been regarded as not suitable for heterogeneous catalysis. Bond and Parvano [3] had done some extensive work regarding the catalysis of gold, and later on that work was reviewed by Wachs and Schwank [3] who then reported that there had been a little use of gold in practical heterogeneous catalysis. Recently gold nanoparticles have been studied and their physical and

chemical properties are very different from the bulk material. The properties of gold nanomaterials depend on both the particle size as well as the particle shape. The strong light absorption in the visible region is shown in gold nanoparticles this is due to the nanoparticles' coherent oscillation of the free electrons on the particle surface which is called the surface plasmon resonance. This surface plasmon resonance effect is one of the best characteristics of gold nanoparticles and include the manner in which they interact with the thiol groups which can be controlled and their non-toxicity. And because of its amazing chemical stability, biocompatibility, and the most distinctive catalytic activity gold nanoparticles have been applied in a broad range of applications in areas that include biomedical research, electronics, information storage and photovoltaic devices. Amongst all the most outstanding examples include cancer diagnosis, molecular ruler, for DNA sequence detection, carbon monoxide oxidation at very low temperatures, as well as thermal and colormetric sensing. These nanoparticles have attracted researchers because of their exceptional optical electronic properties. It has been found that when gold nanoparticles are finely dispersed with particle diameters smaller than 10 nm and supported on a certain metal-oxide semiconductor support, particularly TiO_2, they exhibit a high catalytic activity. It has been reported that Au nanoparticles depend on both size (which must be lower than 5 nm) and the support used. [3,4]

2.2 Synthesis of TiO_2 nanomaterials

Many methods have been used to synthesize TiO_2 nanomaterials, and they include the sol-gel, microemulsion and hydrothermal method. The microemulsion method is expensive and it leads to a small TiO_2 yield. However, the hydrothermal method is low cost , rapid and yields good results when handled correctly.

Sikhwivhilu et al [5] synthesized TiO_2 nanomaterials by the hydrothermal treatment. The authors used TiO_2 (P-25 Degussa) with various bases such as LiOH, NaOH, KOH and NH_4OH. The effect of the base on the morphology transformation of the nanomaterials was investigated. After characterisation the authors observed the presence of tubular and non-tubular structures. Different structures were obtained with the variation of KOH concentration. At the concentration of 18 M KOH, 100% tubular structures were obtained.

Xiong et al [1]synthesized titanate nanotubes via the hydrothermal method. TiO_2 (P-25 Degussa) was treated with 10 M NaOH, the mixture was thoroughly stirred and then autoclaved at 130 ^{0}C for 72 hours. The solid product was washed with ethanol until pH 7 was

reached. The obtained powder was then calcined at 400 ^{0}C for 2 hours. The SEM results showed that the material had a tubular structure. The authors then studied the adsorption and photocatalytic degradation of methylene blue over titanate nanotubes and titanium dioxide, the studies were done for comparison. Titanate nanotubes were found to show higher adsorption ability to methylene blue than titanium dioxide.

Wong et al [6] synthesized titania nanotubes by the hydrothermal method using mild temperatures. The authors then reviewed and analysed the mechanism of titania nanotube formation by this method. The authors further investigated the parameters that affect the formation of titania nanotubes such as the starting material, sonication pretreatment, hydrothermal temperature, washing and calcination processes. The authors finally analysed the effects of the presence of dopants on the formation of titanium dioxide nanotubes. The authors then concluded that in order to enhance the photocatalytic activity of titania nanotubes, optimum conditions are needed to focus on the relationship between the photocatalytic activity and physical properties of TiO_2 nanotubes.

Moghaddam, and Nasirian, [7] synthesized TiO_2 nanostructured materials by the sol-gel method. $TiCl_4$ was used with ethanol. The $TiCl_4$ - ethanol solution was prepared in an argon gas environment, with and without the application of ultrasonic waves. Each sol-gel solution was vaporised at 80 ^{0}C until a dry gel was obtained, and was calcined at 400 ^{0}C for 1 hour until a TiO_2 powder was formed. The XRD confirmed that all the peaks present were anatase phase. The SEM results showed that the use of ultrasonic waves resulted in greater homogeneity in the average size and smaller particles were obtained. The authors then concluded that smaller and more controlled nanoparticles can be produced using ultrasonic waves.

Bavykin et al [8] used the alkaline hydrothermal method for the treatment of different types of TiO_2 structures. TiO_2 (P-25 Degussa) was used with NaOH, KOH, HCl, H_2SO_4 and H_2O_2, (Ti-(O-iPr)$_4$), 25% aqueous solution of NH_3, EtOH, glycerol and NH_4F. The macroporous tubular TiO_2 were first prepared with Ti-(O-i Pr)$_4$ and the NH_3 solution without stirring the macroporous TiO_2 structures, sea urchin shapes and anodic nanotube arrays were prepared and then KOH and NaOH were used to transform the morphology of the materials to nanotubes. The sea urchin shapes were prepared with Ti- (O-IPr)$_4$ and HCl. The anodic nanotube arrays were prepared by anodic oxidation of Ti foil in H_2O-glycerol electrolyte

containing fluoride ions. The above three structures prepared above were then treated with KOH and NaOH in order to transform the morphology. The mixtures were then placed in PFA round-bottomed flask equipped with a thermometer and H_2O jacketed condenser. The HCl was used to wash the samples in order to convert titanate nanotubes into their protonated form. The effect of the size and geometry of these structures on the morphology of the forming agglomerates was investigated. The authors succeded in transforming the spherical morphology to the titanate nanotubes.

Aruna et al [9] synthesized titania nanomaterials using the hydrothermal method . The authors used titanium isopropoxide, isopropanol and a solution of pH 0.5. During the treatment one set was stirred and the other was not. The mixtures were then autoclaved . After characterisation , the TEM results showed that the material that was stirred had smaller particles that were uniform while the unstirred sample showed bigger particles with irregular shapes. The XRD results showed that the stirred samples consisted of pure rutile while the unstirred sample had a mixture of rutile (61%) and anatase (39%). The authors concluded that stirring and aging control the experiment, and most of the TiO_2 condensation occurs during the autoclaving step.. They also concluded that the large colloid particles and the formation of anatase structure in the absence of stirring are due to the inhomogeneity developed in the solution under the extreme conditions of the hydrothermal process.

Li and Wang [10], synthesised TiO_2 nanomaterials by the microemulsion method. They used $TiCl_4$ solution as the titania source and ammonia in reversed microemulsion systems. Two microemulsion systems were prepared, containing 0.5 M $TiCl_4$ aqueous solution and a 2.0 M ammonia. The $TiCl_4$ solution was prepared by adding HCl to H_2O before adding $TiCl_4$ in order to avoid the formation of $Ti(OH)_4$. The microemulsion was formed by mixing the oil phase, surfactant and aqueous phase in a beaker at 13 ^{0}C in a water bath. The obtained powder was white and then it was characterized. The powder was amorphous and then it was calcined at temperatures from 200 to 750 ^{0}C and it transformed to anatase. After heating at a temperatures higher than 750 ^{0}C rutile was formed. Most particles were found to be spherical.

Kasuga et al [11] synthesized titania nanotubes by treating sol-gel derived needle-shaped TiO_2 materials with 5-10 M NaOH for 20 hours at 110 ^{0}C. The needle-shaped products that were produced were subsequently characterized by TEM and BET which revealed that a tubular

structure with a surface area of 400 $m^2.g^{-1}$ .This material showed great potential for use in the preparation of catalysts, adsorbants, and deodorants with high activities.

2.3 Loading of TiO_2 with Au nanomaterials

When titania is doped, in order to obtain a stable and durable materials the metal used should be chemically inert especially towards photo-oxidation and because of this reason noble metals have been used since they suit the purpose. Noble metals such as Pt, Pd, Ag and Au has been used for doping and the photocatalytic activity has been investigated. But Au supported on titanium dioxide has attracted much attention because Au / TiO_2 has been used recently in the field of heterogeneous catalysis and this field has expanded to photocatalysis. Haruta [12] and co workers has done some excellent work on Au / TiO_2 and they found that these nanoparticles can oxidize CO to CO_2 at very low temperatures, and that is very important in pollution control. The best way to improve Au / TiO_2 is to use titania support with a high surface area. Many methods have been employed to synthesize Au / TiO_2 nanoparticles, and they include: reduction of Au nanoparticles in the presence of TiO_2 particles, the sol gel method, the deposition precipitation method, gas- phase grafting, ion implantation, uv- photolysis. Using deposition precipitation method yields the best nanoparticles with the particle size less than 5 nm. And the smaller the particle size, the higher the photocatalytic activity. [12,13,14].

Since the excellent work that was done by Haruta [12] and his co –workers to synthesis Au / TiO_2 nanomaterials, many researchers have done some work to synthesis these materials. The objective of loading titania is to produce stable and durable nanocomposites. The metal used for loading, the dopant, should be chemically inert especially towards photooxidation. Noble metals meet this requirement.

Sonawane and Dongare [15], prepared thin films of Au/TiO_2 by a simple sol- gel method for photocatalytic degradation of phenol in sunlight by using a sol of colloidal Au doped titanium peroxide (Au/TiO_2 sol). The authors started by preparing the colloidal Au/ TiO_2 sol and then the Au/ $Ti0_2$ thin films.. The photocatalytic activity of the thin films was tested by using an in house fabricated quartz reactor. The kinetic study showed that the rate of decomposition of phenol using Au / TiO_2 photocatalysts was improved by 2 to 2.3 times than the undoped TiO_2.

Hernåndes-Fernåndes et al [16] prepared Au/TiO_2 photocatalysts for the oxidation of nitrogen monoxide (NO) in a gas phase by the controlled sol-gel method. Titanium tetraisopropoxide, and $HAuCl_4$ were dissolved in 2-propanol and distilled water. The reaction was prepared under acidic conditions. The evaluation of the photocatalytic activity was performed in-situ by using an FTIR spectrometer with a high sensitivity and UV-VIS spectrometer. The photocatalytic conversion of NO to NO_2 was studied by FTIR , and it reached 85% in 1 hour. The authors then concluded from their results that doping TiO_2 with Au exerts little effect on the band gap. The Au nanoparticles were found to be less than 10 nm.

Wu et al [17] synthesized core-shell Au/TiO_2 nanoparticles by using a simple hydrothermal procedure. The materials (the products) were then characterized by using TEM, HRTEM, XRD and UV – VIS.

Yu, et al [18] prepared the Au/TiO_2 nanocomposite microspheres by the hydrothermal method. Tetrabutyl titanate was mixed with a solution of water, ethanol, Au colloidal particles at 180 °C for 7 hours. The photocatalytic activity was then evaluated by the photocatalytic oxidation decomposition of formaldehyde in air. The authors then concluded from their results that Au nanoparticles slightly depressed the growth of anatase thus resulting in smaller crystallite size and greater specific surface areas. It was again observed that the absorbance and photoluminescence of TiO_2 was modified by Au nanoparticles and that led to an increase in band gap, decrease in photoluminescence intensity and prolonged the life of photo–generated electrons and holes.

Sangeetha et al [19] prepared the Au/ TiO_2 by the deposition-precipitation method, and they used various bases such as NaOH , NH_4OH and urea. A high dispersion of Au and narrow size distribution was obtained.Au / TiO_2 catalysts prepared by using NaOH as a base agent showed higher deposition of Au on the TiO_2 as compared to other base agents and it was found to be a better catalyst. The catalytic activity of these catalysts was then investigated for preferential oxidation of carbon monoxide in hydrogen stream.

Delannoy et al [20], synthesized the Au/TiO_2 nanocomposites by using the incipient-wetness impregnation method. The authors then confirmed that a new gold compound formed upon washing, and it was found to be amino –hydroxo- aquo cationic gold complex .

Narkherde et al [21] synthesized Au/ TiO_2 catalysts by using deposition-precipitation procedure. The conventional deposition precipitation technique was employed for gold encapsulation in the mesoporous TiO_2–MCM-48 matrix. The catalysts exhibited 50% of carbon monoxide conversion to carbon dioxide between 262 and 282 K with good reproducibility.

Bamwenda et al [22] used the deposition-precipitation method to synthesize Au/ TiO_2 for the photocatalytic activity for hydrogen generation. The reagents used were powdered TiO_2, $HAuCl_4$. $4H_2O$, $H_2PtCl_6.6H_20$ and ethyl alcohol. No significant change of Au/ TiO_2 samples was observed after H_2 treatment.

Li et al [23] used deposition- precipitation for preparing Au catalysts supported on TiO_2.The gold amount used should have resulted in a nominal gold loading of 4.48%. Chemical analysis revealed loadings of 1.22% at pH 10 that is, the gold was not completely precipitated onto the support. The gold loading was somewhat higher at lower pH (1.62% at pH 8 as compared to 2.06% at pH 7). Reproducible catalysts were obtained.

Anandan and Ashokkumar [24] prepared the $Au/Ti0_2$ photocatalysts sonochemically by three different procedures. The photocatalytic and sonophotocatalytic efficiencies of the prepared materials were evaluated by studying the degradation of a representative organic pollutant nonyl phenol ethoxylate (NPE) surfactant in aqueous solution.

2.4 References

1. Xiong L., Sun W., Yang, Y., Chen C. and Ni J. (2011). **Heterogeneous photocatalysis of methylene blue over titanate nanotubes : Effect of adsorption.** Journal of Colloid and Interface science, **356**, 211-216.

2. Primo, A., Corma, A., and Garcia, H. (2010). **Titania supported gold nanoparticles as photocatalyst**. Institution de Tecnologia Quimica , Universidad Politecnica de Valencia-CSIC, Camino de Vera,46022 Valencia, Spain.

3. Haruta M. (1997). **Size- and support- dependency in the catalysis of gold**. Catalysis Today, **36**, 153- 166.

4. Měndez- Cruz M., Ramĺrez- Solis J. and Zanella R. (2011). **CO oxidation on gold nanoparticles supported over titanium oxide nanotubes.** Catalysis Today, **166**, 172- 179.

5. Sikhwivhilu, L.M, Sinha Ray, S, and Coville, N.J.,(2009).**Influence of bases on hydrothermal synthesis of titanate nanostructures**. Applied Physics A Materials science and processing, **94**, 963-973.

6. Wong, C.,L., Tan, Y.N., and Mohamed, A.R. (2011). **A review on the formation of titania nanotube photocatalysts by hydrothermal treatment.** Journal of Environmental Management, **92**, (1669-1680).

7. Moghaddam, H.M. and Nasirian, S. (2011). **Ultrasonic wave effects on the diameter of TiO_2 nanoparticles**. S. Afr. J. Sci, 107 (3/4).

8. Bavykin, D.V., Kulak, A.N. and Walsh, F.C. (2011). **Control of Hierarchical Structure of Titanate Nanotube Agglomerates.** Langmuir, **27**, 5644 – 5649.

9. Aruna, S.T., Tirosh, S. and Zaban, A. (2000). **Nanosize rutile titania particle synthesis via a hydrothermal method without mineralizers**. J. Mater. Chem., **10**, 2388-2391.

10. Li, G.L. and Wang, G.H. (1999). **Synthesis of nanometer – sized TiO_2 particles by a Microemulsion method.** Nanostructured Materials, **11**(5), 663 – 668.

11. Kasuga, T., Hiramatsu, M., Hoson, A., Sekino, T. and Niihara, K. (1998). **Formation of titania nanotubes**. Langmuir, **14**, 3160-3163.

12. Sau, T.K., Pal, A., Jana, N.R., Wang, Z.L. , and Pal, T.(2001). **Size controlled synthesis of gold nanoparticles using photochemically prepared seed particles.** Journal of Nanoparticles Research, **3**, 257 – 261.

13. Molina, L.M., Rasmussen, M.D and Hammer, B. (2004). **Adsorption of O_2 and oxidation of CO at Au nanoparticles supported by TiO_2 (110).** Journal of Chemical Physics, **120** (16), 7673-7680.

14. Měndez- Cruz M., Ramĺrez- Solis J. and Zanella R. (2011). **CO oxidation on gold nanoparticles supported over titanium oxide nanotubes.** Catalysis Today, **166**, 172- 179.

15. Sonawane, R.S. and Dongare, M.K. (2006). **Sol-gel synthesis of Au / TiO_2 thin films for photocatalytic degradation of phenol in sunlight.** Journal of Molecular Catalysis A : Chemical, **243**, 68-76.

16 .Herna´ndez-Ferna´ndez, J., Aguilar-Elguezabal, A. Castillo, S., Ceron-Ceron, B. Arizabalo, R.D. and Moran-Pineda, M. (2009). **Oxidation of NO in gas phase by Au – TiO_2 photocatalysts prepared by the sol-gel method.** Catalysis Today, **148**, 115-118.

17. Wu, X.-F., Song, H.-Y., Yoon, J.-M., Yu, Y.-T., and Chen, Y.-F. (2009). **Synthesis of core-shell Au/$Ti0_2$ nanoparticles with truncated wedge-shaped morphology and their photocatalytic properties.** Langmuir, **25** (11), 6438-6447.

18. Yu, J., Yue, L., Liu, S., Huang, B. and Zhang, X. (2009). **Hydrothermal preparation and photocatalytic activity of mesoporous Au/TiO_2 nanocomposite microspheres**. Journal of Colloid and Interface Science, **334** (1), 58-64.

19. Sangeetha , P., Chang, L., and Chen, Y. (2009). **Gold catalysts on TiO_2 support for preferential oxidation of CO in hydrogen stream : Effect of base agent.** Materials Chemistry and Physics, **118** (1), 181-186.

20. Delannoy, L., El Hassan, N., Musi, A., Le To, N.N., Krafft, J.-M. and Louis, C. (2006). **Preparation of supported Au nanoparticles by a modified incipient**

wetness impregnation method. Journal of Physical chemistry B, **110** (45), 22471-22478.

21. Narkhede, V.S., De Toni, A., Narkhede, V.V., Guraya, M., Niemantsverdriet, J.W., Van der Berg, M.W.E., Grünert, W. and Gies, H.(2009). **Au/TiO_2 catalysts encapsulated in the mesopores of siliceous MCM-48- Reproducible synthesis, structural characterization and activity for CO oxidation.** Microporous and Mesoporous materials **118** (1- 3), 52-60.
22. Bamwenda, G.R., Tsubota, S., Nakamura, T. and Haruta, M. (1995). **Photoassisted hydrogen production from a water- ethanol solution: a comparison of activities of Au/TiO_2 and Pt/TiO_2.** Journal of Photochemistry and Photobiology A: Chemistry, **89**, 177-189.
23. Li, X.W., Hu, Y.M and Wang,Z.G.(1998).**Investigation of dislocation structure in a cylically deformed copper single crystal using electron channeling contrast technique in SEM**. Materials Science and Engineering A, **248**(1-2),299-303.
24. Anandan , S. and Ashokkumar, M. (2009).**Sonochemical synthesis of Au/TiO_2 nanoparticles for the sonophotocatalytic degradation of organic pollutants in aqueous environment.** Ultrasonics Sonochemistry, **16** (3), 316-320.

CHAPTER 3

3.1 Introduction

Au / TiO_2 nanomaterials have been successfully prepared using different methods. The TiO_2 support is always prepared first and then the loading of Au follows. These nanomaterials possess very unique and important properties that are more dependent on the size and shape of the material. The preparation of the nanomaterials that possess the required size and shape has been the focus of research in the field of nanotechnology, and it is not a very simple task to produce materials that are stable with controlled size. Therefore there is a need to develop a new general method and to improve the existing methods. The reason for the use of TiO_2 as the best support is driven by the fact that it is the best semiconductor and it is reducible. Methods such as the hydrothermal method, sol–gel method and microemulsion are the most common in the preparation of the TiO_2 support. Whereas incipient wetness impregnation, deposition–precipitation, co-precipitation and deposition are employed for loading Au on the TiO_2 support[1,2,3].

3.2 Chemicals and reagents

KOH, NaOH, TiO_2 (P- 25 Degussa), NH_4OH (33 %), $HAuCl_4.3H_2O$ .These chemicals were of analytical grade and they were purchased from either Merck, Sigma-Aldrich or Riedel-de Haën. Deionised water was used for all the experiments.

3.3 Equipments

An autoclave, model PARR 4843 , was used with a stirring rate of 500 rpm and a temperature of 150^0C for 24 hours. This was done for all the experiments. After 24 hours it is very important to always release the pressure from an autoclave and allow the sample to cool before you remove it.

A centrifuge, model Allegra X 22R from Beckmann Coulter was used to separate the solid from the mixture. The stirring speed was 4500 rpm and the rotor of 4250 with an acceleration of 9 and a temperature of 4 ^{0}C for 10 minutes were employed. The solid was washed with deionized water until the conductivity of the supernatant liquid was less than 100 μS/cm.

A conductivity meter was employed to check the conductivity of the mixture.

The samples were then vacuum-dried for ± 14 hours in an oven at 100 °C.

The obtained powder was then characterized by scanning electron microscopy (SEM), transmission electron microscopy (TEM), Energy dispersive x-ray (EDX) spectroscopy, x-ray diffraction (XRD), Brunauer- Emmett-Teller (BET) method and fourier transform infrared (FTIR) spectroscopy. After characterization the samples were then calcined at 300^0C for 4 hours in a furnace, model Lenton from Elite Thermal Systems Limited. The calcination was done to make the samples crystalline and to remove volatile substances.

3.4 Methods of synthesis of TiO_2 support

3.4.1 Hydrothermal method

This method is the synthesis method of single crystals that depend on the solubility of chemicals in high temperatures under high pressure. The hydrothermal phase equilibrium is the theory that was first studied by the geochemists and mineralogists since the last century, and that makes the hydrothermal technique to be of geologic origin. The hydrothermal method has been previously reported to be a very effective synthesis tool for the synthesis of nanomaterials, and this method is very important during the processing of monodispersed and highly homogeneous nanoparticles. Since it has the advantage of preparing the nanomaterials for a wide variety of applications, it has become one of the most important tools for the processing of advanced materials. Nanostructures can be synthesized by simply controlling the grain size, morphology of particles, the crystalline phase and the surface chemistry and this can be achieved by adjusting factors such as the composition of the sol, pH, reaction temperature, pressure, aging time and nature of the solvent . But this method was originally designed for the single- growth of particles such as various mechanisms for crystallizing substances from high-temperature aqueous solutions at high pressures. Hydrothermal synthesis usually takes place in a steel pressure vessel which is called an autoclave, and it is often referred to as the pressure cooker. For the crystal to grow, the temperature-gradient has to be maintained at opposite ends of the growth chamber, for the hotter end to dissolve the nutrient whereas the cooler end causes the seeds to grow. This method is advantageous in that it has the ability to create crystalline materials that are unstable at their melting points, and it can produce materials with high vapor pressure near their melting points. For example, some materials are insoluble in water but at high temperatures and high pressures they become soluble. TiO_2 nanomaterials with different morphologies have been yielded under various

hydrothermal conditions. This method can yield well crystalline anatase titania nanoparticles which are uniform and well dispersed. In the industries it is the most excellent among the solution phase techniques because it is low cost and rapid. [4,5,6,7].

3.4.2 The sol-gel method

This method is versatile and has been employed in the production of a variety of materials with photonic, electronic, mechanical, chemical, biological and biomedical properties. It can be used to produce important materials by carefully improving the processing method. The sol-gel method is considered to be amongst the important methods used in the production of materials with novel properties, and it is one of the resourceful methods for the preparation of metal oxide nanomaterials such as TiO_2 nanomaterials. When this technique is employed in the synthesis of TiO_2 nanomaterials, usually it involves the hydrolysis and the condensation of titanium alkoxides to produce oxopolymers which can then be transformed into an oxide network. By simply tailoring the chemical structure of the primary precursor and by controlling the processing variables carefully, nanomaterials with high level of purity can be obtained. The sol-gel technique allows flexibility in parameter control with its relatively slow reaction process since it is a solution method. Therefore, tailoring of certain desired structural characteristics such as compositional homogeineity, grain size, particle morphology and porosity is permitted. By simply controlling the hydrolysis and condensation steps carefully, the constituent materials can be homogeneously mixed easily at the molecular level. The disadvantage of this method in the synthesis of TiO_2 nanomaterials is that it yields the amorphous phase which then needs to be calcined at higher temperatures and that can lead to particle agglomeration and reduced surface area [8,9,10,11].

3.4.3 Microemulsion method

The microemulsion method is a very promising technique in the preparation of nanometer-sized materials and is currently an area that has attracted much interest. Microemulsions have gained increasing importance in both basic research and different industrial fields, owing to their novel properties that include ultra low interfacial tension, large interfacial area, thermodynamic stability and their ability to solubilize immiscible liquids. Microemulsions are mostly used and applied in both chemical and biological fields. This method has a wide range of applications such as oil recovery and in the synthesis of nanoparticles. The nanomaterials that have been synthesized by this method have resulted in significant

applications such as catalysts, high performance ceramic materials, microelectronic devices, high-density magnetic recording and in drug delivery. This technique is regarded to be amongst the versatile preparation methods, as it enables the control of particle properties such as size, geometry, morphology, surface area and homogeneity of the material. The microemulsion method has been previously employed in the preparation of colloidal metals such as colloidal Fe_3O_4 , and colloidal AgCl, and it has also been used in the preparation of nanocrystalline materials such as Fe_2O_3, TiO_2 and Al_2O_3. However, when it comes to the synthesis of TiO_2 nanomaterials this method is expensive, since the ratio of the aqueous phase to oil phase and surfactant in these systems is very small and this leads to a small amount of TiO_2 yield [12,13,14].

3.5 Methods of synthesis of Au / TiO_2 nanocomposites

Nanocomposite materials is a newly emerging area of materials and they are obtained by tuning the molecular level interactions of different components to form new, unique materials with improved properties. Generally, nanocomposite materials are produced by introducing the filler into the matrix. These materials exhibit extremely improved properties such as strength, modulus, dimensional stability, chemical and thermal stability, permeability for gases, water and hydrocarbons, electrical and thermal conductivity, surface properties, optical properties and dielectric properties. Nanocomposites doped with semiconductors have been widely studied due to their unique improved properties [15,16,17].

3.5.1 Incipient wetness impregnation

This is amongst the most well known techniques used to prepare catalysts supported on noble metals. $HAuCl_4$ is the most common precursor and source of Au. This technique often leads to the formation of large Au particles after post-thermal treatment. These large particles arise from the presence of chloride ions. This method works very well with any type of metal-oxide combinations even at low metal loadings [18,19].

3.5.2 Deposition – Precipitation (DP) method

This method is one of the most common techniques often employed in the synthesis of Au / TiO_2 nanomaterials for various applications such as catalysis and CO oxidation. Haruta [20] has proved that by using this method, you can actually obtain Au nanomaterials with an average particle size of about 5 nm. The Au / TiO_2 nanomaterials that are synthesized by this

method have proved to be very active. When this method is employed, the most important parameter is the pH value because it controls the speciation of Au^{3+}. $HAuCl_4$ is also the most common precursor that is usually employed. Firstly, the pH of $HAuCl_4$ has to be adjusted in the range of 6 – 10 and then the metal oxide support is immersed into the solution, and then the solution has to be aged for at least 1 hour in order to allow the deposition of $Au(OH)_3$ on the support. Adjusting the pH is very important as it plays a very huge role on the particle size[20,21].

3.5.3 Co-precipitation

This method is one of the most versatile techniques because it can yield stable precursor powders on large scale without the use of a special apparatus. It is a very common method in the processing of mass-produced fine powders. Co- precipitation was first employed in obtaining gold nanoparticles in 1987. It was done by the addition of sodium carbonate to an aqueous solution of $HAuCl_4$ and a metal nitrate that led to the production of the support. The coprecipitates were washed and calcined in air. The high gold dispersion with particles having a diameter less than 10 nm has been obtained by this synthesis route and the oxide surface areas which are larger than the ones obtained in the absence of gold can be achieved. This technique works only for certain metal oxides, since the rates of precipitation of the two precursors and their attraction is the important key in the determination of gold nanoparticles size [22,23,24].

3.5.4 Photodeposition

This is one of the alternative methods to prepare titania supported gold nanoparticles. The method gives good results when the support is a semiconductor typically TiO_2. When the semiconductor is irradiated with light of an appropriate wavelength, it produces the photogeneration of electrons and holes, and these electrons can be used in the reduction of gold tetrachloroaurate to gold metal and they will be deposited on the surface of the semiconductor simultaneously. An alcohol has to be used in order to avoid the positive charge accumulation (TiO_2) during this method. This technique has been employed in the preparation of gold nanoparticles supported on titania nanofibers. The typical average Au particle size yielded by this method is between 10 and 30 nm in diameter which is very large for many purposes such as catalysis. The intensity of the light is a very important parameter when using this method [11].

3.6 Characterization of Au / TiO_2 nanomaterials

Characterization refers to the use of a technique to investigate and determine the physical, chemical and mechanical properties of a material. Because the characteristics of a particle can impact the quality and performance of the objects, the particles need to be characterized. The characterization of particles is important in research and development, and in the manufacture and quality control of materials and products. Characterization is an important tool in scientific research. It is important for materials scientists to be able to characterize the microstructure of materials because they can quantify the properties and anticipate the capability of a material to perform well in a given application. Chemical characterization helps in identifying and quantifying the chemical constituent of a material.

Characterization of nanomaterials is challenging because of the difficulties in determining structures of such small size therefore , different characterization techniques are used and they include the following: scanning electron microscopy (SEM), transmission electron microscopy (TEM), x-ray diffraction (XRD) ,Brunauer Emmett Teller method (BET), ultraviolet (UV) spectroscopy and fourier transform spectroscopy (FTIR) [25,26,27].

3.6.1 Scanning electron microscopy (SEM)

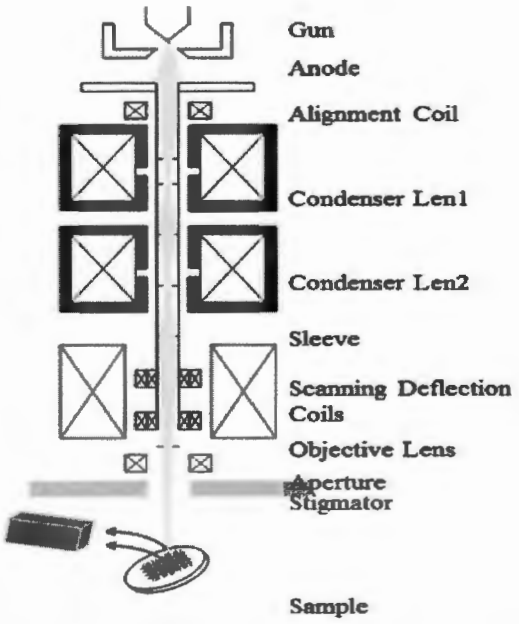

Figure 3.1: A schematic representation of a scanning electron microscope [28]

SEM is by far the most versatile instrument available in the examination and the analysis of the microstructural characteristics of solid objects owing to its high resolution. This microscope can image and analyse bulk specimens. The large depth of field is partly responsible for the appearance of an image that is 3-dimensional. With this technique it is possible to examine objects using a low magnification. Commercially available SEM instruments possess the instrumental resolution on the order of 1–5 nm which is recommended. The typical SEM instrument consists of the lens system, the electron gun, the electron collector, the visual and photoreading cathode ray tubes [8]. During SEM analysis, the electron beam scans through the surface of the sample and that results into the production of a huge amount of signals. These signals are eventually converted to the image [29]. The SEM instrument that has the low voltage that ranges from 0.1 to 5 keV is also referred to as the low voltage SEM (LVSEM). For the virtual source , the smallest beam cross-section at the gun has a diameter that follows the order of 10 - 50 μm and the diameter of 10 – 100 nm in the case of field emission guns. This beam is then demagnified by using a 2 or 3 stage electron lens system that allows the electron probe with a diameter of 1-10 nm consisting of electron - probe current in the range 10^{-9} to 10^{-12}A that occurs at the specimen surface. In the case of the operation that utilizes an electron – probe current that is a bit higher, which is approximately 10^{-8} A there is an increase in the probe diameter to approximately 0.1 μm [,30,31,32].

3.6.2 Transmission electron microscopy (TEM)

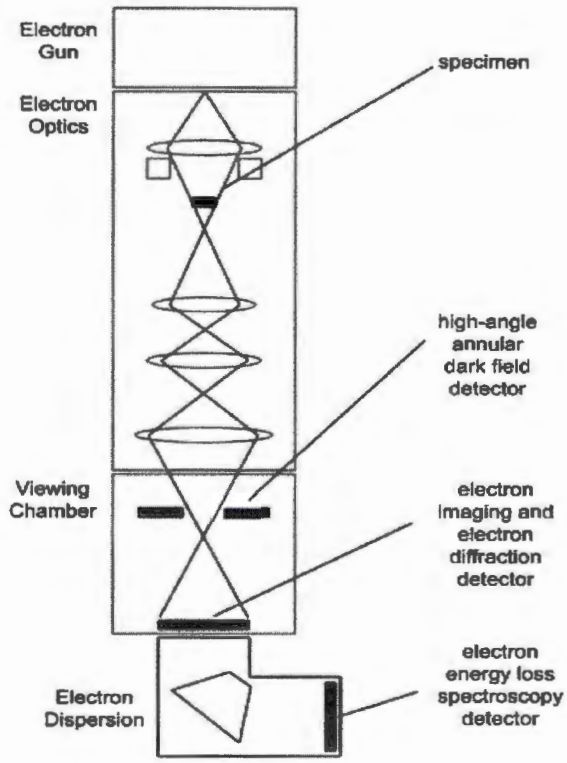

Figure 3.2: A schematic representation of a of a transmission electron microscope [33]

Transmission electron microscopy (TEM) is used as a major research tool, and it is the only analytical instrument that can provide microstructural details of metals and their alloys directly with their physical, chemical, and mechanical properties at the atomic level. Since this technique uses more powerful electron beams than SEM, its high resolution provides greater detail of materials in terms of crystallinity and granularity at the atomic scale [34]. In electron microscopes (TEM, SEM), the electrons are used instead of photons since electrons have a shorter wavelength than photons, and this is why it is possible for the observation of matter at the atomic scale. For the TEM analysis, thin samples are needed, since the electrons in the material have to be absorbed. Ernst Ruska and Max Knoll [35] were the first to obtain the TEM image. The TEM microscope utilizes electrons that are usually accelerated at a high voltage to a velocity that approaches the speed of light. Typical TEM analysis involves the irradiation of a sample with an electron beam that possesses uniform current density. The acceleration voltage that is used routinely on instruments ranges from 100 – 200 kV for a

normal TEM. In case of medium–voltage instruments a voltage of 200 – 500 kV is required for better transmission and resolution, whereas a high–voltage microscope has an acceleration voltage of 500 kV- 3mV. During characterization, there occurs an emission of electrons in the electron gun by thermionic and field emission [35]. In this case a 3 or 4 stage condenser lens system is required in order for the area of the specimen that is illuminated and the variation of the illumination aperture to be permitted. To observe the electron- density distribution that is behind the specimen, a lens system is used for the imaging and it usually consists of 3 to 8 lenses that display onto the fluorescent screen. There are many ways for the image to be recorded. It could be by direct exposure of an image plate that is inside the vacuum or by digitally displaying the fluorescent screen coupled by a fiber- optic plate to a camera. There is a strong interaction of electrons with atoms by elastic and inelastic scattering [36].

3.6.3 X- ray diffraction (XRD)

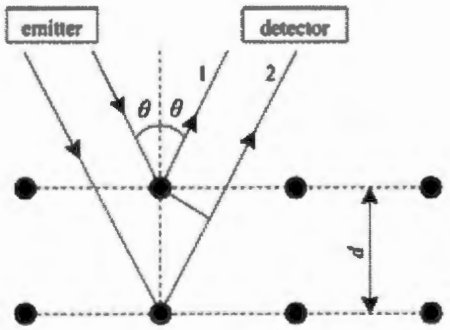

Figure 3.3 : A schematic representation of an x-ray diffractometer [37]

X–ray diffraction (XRD) measurements are widely used and applied in the study, identification and monitoring of the crystalline structure of materials, particularly in fine grained samples and various experimental configurations [38]. This technique gives information of the particle size and it is able to identify crystalline phases [39]. It is the most commonly used technique for quantitative analysis. This technique is based on the fact that the intensities of the diffraction lines are proportional to the amount of the crystal phase [40] .One of the important advantages of XRD is that it is possible to perform a study while the catalyst is in its working environment [41]. The crystallite size of the sample is estimated by using the Debye-Scherrer equation:

$$S = K\lambda / (\beta \cos\theta) \qquad (1.1)$$

Where S is the crystallite size, λ is the wavelength of the x-ray, K is a constant, β is the line width at half maximum height and θ is the diffraction angle [42].

3.6.4 Brunauer –Emmett - Teller (BET) method

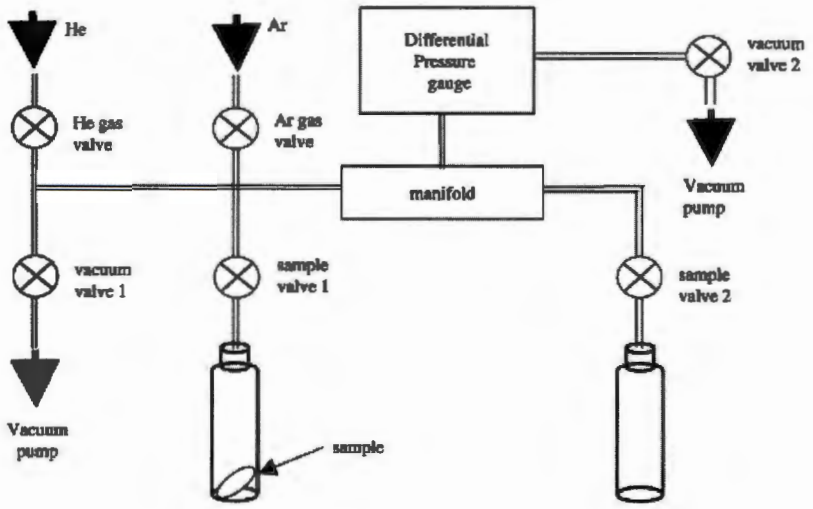

Figure 3.4 : A schematic representation of a Brunauer Emmett Teller [43]

In the characterization of novel porous materials, the surface area is one of the most important quantities. The BET analysis is the best method to determine the surface areas from nitrogen- adsorption isotherms. It was originally derived for multilayer gas adsorption onto flat surfaces. The surface areas are commonly referred to as BET surface areas since they are obtained by simply applying the Brunauer, Emmett, and Teller theory to nitrogen adsorption isotherms usually materials measured at 77 K. This is a very standard method as it allows for comparisons among different materals. This procedure assumes that adsorption occurs by multilayer formations and that the number of layers that are adsorbed is infinite at the saturation pressure. It simply means that it assumes that the materials adsorption occurs as if they are on a free space.

The term adsorption was firstly introduced by Kayser [44] to describe the increase in the concentration of gas molecules in neighbouring solid surfaces in 1881. And it was a phenomenon that was noted by Fontana and Scheele [44]. Kayser then suggested the first empirical formula of the adsorption isotherm:

$$V = a + bP \qquad (1.2)$$

Where V is the adsorbed volume of a gas related to the volume of a sample, P is the pressure in torr and a and b are the temperature dependent constant.

Ostwald [44] introduced the term adsorption isotherm. McBain [44] was the first to separate the phenomena of adsorption and absorption. The first theoretical equation of adsorption isotherm was derived by Langmuir. Brunauer, Emmett and Teller used the derivation of the Langmuir isotherm to derive the BET adsorption isotherm which is also known as the Brunauer-Emmett-Teller (BET) adsorption isotherm[45,46].

3.6.5 Fourier transform infrared spectroscopy (FTIR)

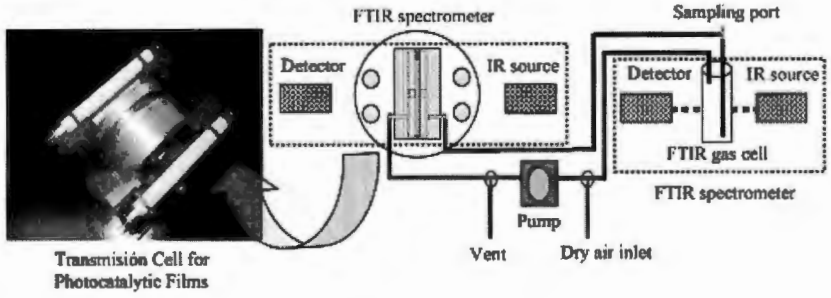

Figure 3.5: A schematic representation of a fourier transform infrared spectrometer [47]

Fourier transform infrared spectroscopy (FTIR) is one of the most versatile characterization methods. It has significant advantages over the dispersive system infrared technique. It has been used by chemists as a powerful tool. This technique is able to provide information about the chemical bonding of organic and inorganic materials. During FTIR analysis, IR beam is passed through the sample, some of this radiation is absorbed by the sample and some is transmitted. The transmittance and reflectance of the sample of the infrared rays at different frequencies is then translated to an infrared absorption plot. This Infrared spectrum of a compound is known to give exclusive "fingerprint". FTIR offers reliable information about aliphaticity, aromaticity, and oxygenation rate and it can give more accurate data such as the average distribution length of aliphatic chains, oxygenation and substitution modes of aromatics. It is also applicable in evaluating the efficiency of antiviral drugs [,48,49,50].

3.6.6 Ultraviolet – Visible spectroscopy (UV/ VIS)

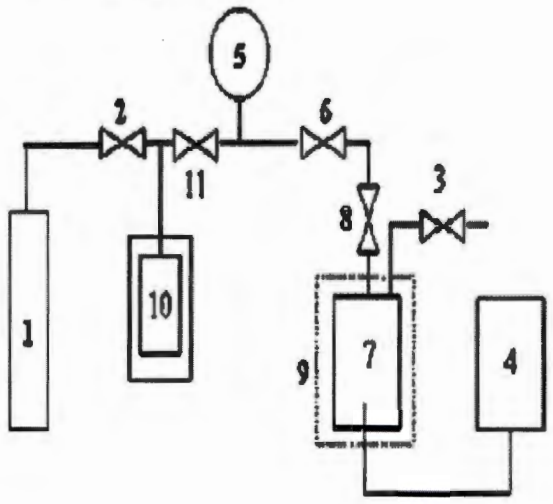

Figure 3.6 : A schematic representation of an ultraviolet- visible spectrometer [51]

Ultraviolet–visible (UV/VIS) spectroscopy is one of the oldest and simplest forms of spectroscopy for analyzing the biological macromolecular structure. Since UV is the spectroscopy of photons in the UV and VIS region, the electromagnetic radiation generated by an ultraviolet spectrometer ranges from 200 to 800 nm. In this region of the electromagnetic spectrum, molecules undergo electronic transitions. The instrument then scans this range and the absorption spectrum is displayed on a computer screen with the relative absorbance on the vertical scale (0 to 1.0) and the wavelength on the horizontal scale. First the sample is dissolved in a solvent and placed in a cell that does not absorb in the targeted UV region. A reference cell containing only the solvent is used and the absorbance, A, of the sample is reported as the log of the ratio of the beam intensity of the incident light, I_O , divided by the intensity of the light, I, that is transmitted through the samples. A is also proportional to the sample concentration, c, the length or thickness of the sample cell, and the molar absorptivity, ε, which is also called the extinction coefficient and is calculated from the equation. And this can be represented as an equation called the Beer–Lambert law : [52,53,54]

$$A = \log \frac{I_O}{I_{sample}} = \varepsilon \, l \, c \qquad (1.3)$$

The Beer–Lambert law is valid for dilute solutions [55].

3.7 References

1. Venkatachalam, N., Palanichamy, M. and Murugesan, V. (2007). **Sol gel preparation and characterization of alkaline earth metal doped nano TiO_2 : Efficient photocatalytic degradation of 4- chlorophenol.** Journal of Molecular Catalysis A: Chemical, **273**(1-2), 177-185.
2. Sau, T.K., Pal, A., Jana, N.R., Wang, Z.L. , and Pal, T.(2001). **Size controlled synthesis of gold nanoparticles using photochemically prepared seed particles.** Journal of Nanoparticles Research, **3**, 257 – 261.
3. Molina, L.M., Rasmussen, M.D and Hammer, B. (2004). **Adsorption of O_2 and oxidation of CO at Au nanoparticles supported by TiO_2 (110).** Journal of Chemical Physics, **120** (16), 7673-7680.
4. Byrappa, K. and Adshiri, T. (2007). **Hydrothermal technology for nanotechnology.** Progress in Crystal Growth and Characterization of Materials, **53** (2), 117-166.
5. Liu, J., Ma, J., Liu, Y., Song, Z., Sun, Y., Fang, J. and Liu, Z. (2009). **Synthesis of ZnS nanoparticles via hydrothermal process assisted by microemulsion technique**. Journal of Alloys and Compounds, **486** (1-2), L40-L43.
6. Sahoo, T., Kang, E., Kim, M., Kannan, V., Yu, Y, Shin, D., Kim, T. and Lee, H. (2008). **Growth of ZnO thin film on p- GaN/ sapphire (0 0 0 1) by simple hydrothermal technique.** Journal of Crystal Growth, **310** (3), 570-574.
7. Wong, C.,L., Tan, Y.N., and Mohamed, A.R. (2011). **A review on the formation of titania nanotube photocatalysts by hydrothermal treatment.** Journal of Environmental Management, **92,** (1669-1680).
8. Kuang, Q., Lin, Z., Lian, W., Jiang, Z., Xie, Z., Huang, R. and Zheng, L. (2007). **Synthesis of rare- earth metal oxide nanotubes by the sol gel method assisted with porous anodic aluminium oxide templates.** Journal of Solid State Chemistry,**180**(4), 1236-1242.
9. Su, C., Hong, B.-Y., and Tseng, C.-M. (2004). **Sol gel preparation and photocatalysis of titanium dioxide.** Catalysis Today, **96** (3), 119-126.

10. Sakka, S. (2005). **Handbook of sol gel science and Technology : Applications of sol gel technology.** Kluwer Academic Publishers.

11. Primo, A., Corma, A., and Garcia, H. (2010). **Titania supported gold nanoparticles as photocatalyst**. Institution de Tecnologia Quimica , Universidad Politecnica de Valencia-CSIC, Camino de Vera,46022 Valencia, Spain.

12. Zhang, B. (2008). **Lead chalcogenide nanocomposites : synthesis, thermal and electrical.** Clemson University. Department of Physics. pp 210.

13. Malik, M.A., Wani, M.Y. and Hashim, M.A. (2010). **Microemulsion method: A novel route to synthesize organic and inorganic nanomaterials.** Arabian Journal of Chemistry. ARTICLE IN PRESS.

14. Li, G.L. and Wang, G.H. (1999). **Synthesis of nanometer – sized TiO_2 particles by a Microemulsion method.** Nanostructured Materials, **11**(5), 663 – 668.

15. Pushpakanth, S., Srinivasan, B., Sreedhar,B. and Sastry,T.P. (2008). **An in situ approach to prepare nanorods of titania- hydroxyapatite (TiO_2- HAp) nanocomposite by microwave hydrothermal technique.** Materials Chemistry and Physics, **107** (2-3), 492-498.

16. Hammer,N., Kvande,I., Xu,X., Gunnarson,V., TØtdal,B., Chen,D. and RØnning,M. (2007). **Au/TiO_2 catalysts on carbon nanofibres prepared by deposition-precipitation and from colloid solutions.** Catalysis Today, 123, 246-256.

17. Savage, N., Diallo, M., Duncan, J., Street, A. and Suzan, R. (2009). **Nanotechnology Applications for Clean Water.** William Andrew Inc., Norwich, New York, pp 49.

18. Deng, W. (2008). **The catalytic activity of gold clusters on oxide supports for the low – temperature oxidation of CO by dioxygen and water in hydrogen-rich gas streams.** ProQuest Information and Learning Company, Tufts University, Chemical and Biological Engineering, pp 28.

19. Delannoy, L., El Hassan, N., Musi, A., Le To, N.N., Krafft, J.-M. and Louis, C. (2006). **Preparation of Supported Gold Nanoparticles by a Modified Incipient Wetness Impregnation Method.** J. Phys. Chem. B, **110,** 22471-22478.

20. Haruta M. (1997). **Size- and support- dependency in the catalysis of gold.** Catalysis Today, **36,** 153- 166.

21. Měndez- Cruz M., Ramĺrez- Solis J. and Zanella R. (2011). **CO oxidation on gold nanoparticles supported over titanium oxide nanotubes.** Catalysis Today, **166,** 172- 179.

22. Wang, H., Gao, L. and Niihara, K. (2000). **Synthesis of nanoscaled yttrium aluminium garnet powder by the co - precipitation method.** Materials Science and Engineering: A, **288** (1), 1-4.

23. Li, X., Liu, H., Wang, J., Cui, H., Zhang, X. and Han, F. (2004). **Preparation of YAG : Nd nano-sized powder by co - precipitation**. Materials Science and Engineering: A, **379** (1-2), 347-350.

24. Zhang, B. (2008). **Lead chalcogenide nanocomposites : synthesis, thermal and electrical.** Clemson University. Department of Physics. pp 210.

25. Groeber, M.A., Haley, B.K., Uchic, M.D., Dimiduk, D.M. and Ghosh, S. (2006). **3D reconstruction and characterization of polycrystalline microstructures using FIB- SEM system.** Materials Characterization, **57** (4-5), 259-273.

26. Mulder, M. (1996). **Basic Principles of Membrane Technology**, 2nd Edition. Kluwer Academic Publishers Chap4, pp 158

27. Xu, R. (2001). **Particle characterization : Light scattering methods**. Particle Technology Series. Kluwer Academic Publishers Chap1, pp 1.

28. Jung, K.O,Kim, D.H.,and Kim, S.J.(2012). **An approach to reducing the distortion caused by vibration in scanning electron microscope images.** Nuclear Instruments and Methods in Physics Research A, **676,** 112-120.

29. Zhou, W., Apkarian, R.P., Wang, Z.L. and Joy, D. (2007). **Fundamentals of Scanning Electron Microscopy.** Springer, pp. 1-40.

30. Kowalewska,M. and Szwedo,J. (2009). **Examination of the Baltic amber inclusion surface using SEM techniques and X-ray microanalysis.** Palaeogeography , Palaeoclimatology, Palaeoecology, **271** (3-4), 287-291

31. Poole, I. and Lloyd, G.E. (2000). **Alternative SEM techniques for observing pyritised fossil material.** Review of Palaeobotany and Palynology, **112** (4), 287-295.

32. Lagattu,F., Bridier, F., Villechaise, P. and Brillaud, J.(2006). **In-plane strain measurements on a microscopic scale by coupling digital image correlation and an in situ SEM technique**. Materials characterization, **56** (1),10-18.

33. Moldovan, G., Li, X., Wilshaw, P. and Kirkland, A. (2008). **Thin Silicon strip devices for direct electron detection in transmission electron microscopy.** Nuclear Instruments and Methods in Physics Research A, **591**, 134-137.

34. Nakahara, S. (2003). **Recent development in TEM specimen preparation technique using FIB for semiconductor devices.** Surface and coatings Technology, **169-170** , 721-727

35. Ůnlů, N.(2008). **Preparation of high quality AI TEM specimens via a double-jet electropolishing technique.** Materials characterization, 59(5), 547-553

36. Minakshi, M.(2008). **Examining manganese dioxide electrode in KOH electrolyte using TEM technique.** Journal of Electroanalytical chemistry, **616**(1-2), 99-106

37. Wu, X. and Liu, Z. (2012). **A smoothing method for x-ray spectrum based on best beamforming.** Radiation Physics and Chemistry, **81**, 248 – 252.

38. Ryan P.C., Wall, A.J., Hillier, S. and Clark,L. (2002). **Insights into sequential chemical extraction procedures from quantitative XRD : a study of trace metal partitioning in sediments related to frog malformites.** Chemical Geology,**184** (3-4),337-357.

39. Thamaphat, K., Limsuwan, P. and Ngotawornchai, B. (2008). **Phase Characterization of TiO_2 Powder by XRD and TEM.** Kasetsart J. (Nat. Sci), **42**, 357-361.

40. Sharma, A., Kyotani, T and Tomita, A.(2000). **Comparison of structural parameters of PF carbon from XRD and HRTEM techniques.** Carbon,**38**(14), 1977-1984.

41. Štefanić , G., Molčanov, K. and Musič, S.(2005). **A comparative study of the hydrothermal crystallization of HfO_2 using DSC/TG and XRD analysis.** Materials Chemistry and Physics,**90** (2-3),344-352.

42. Moghaddam, H.M. and Nasirian, S. (2011). **Ultrasonic wave effects on the diameter of TiO_2 nanoparticles**. S. Afr. J. Sci, 107 (3/4).

43. Park, M.S. and Yoon, W.Y. (2003). **Characteristics of a Li / MnO_2 battery using a lithium powder anode at high-rate discharge.** Journal of Power Sources, **114,** 237-243.

44. Rouquerol, J., Rodríguez-Reinoso, F., Sing, K.S.W. and Unger, K.K.(1994). **Characterisation of Porous Solids III.** Elsevier Science B.V.

45. Virkutyte, J., Varma, R.S., and Jegatheesan, V. **Treatment of Micropollutants in water and waste water.**

46. Walton, K.S. and Snurr, R.Q. (2007). **Applicability of the BET method for determining surface areas of microporous metal- organic frameworks.** J. AM. CHEM. SOC., **129**, 8552-8556.

47. Hernández-Alonso, M.D., Tejedor-Tejedor, I., Coronado, J.M., Anderson, M.A.and Soria, J. (2009). ***Operando*** **FTIR study of the photocatalytic oxidation of acetone in air over TiO_2-ZrO_2.**Catalysis Today, **143**, 364-373.

48. Almeida, E., Balmayore, M. and Santos, T. (2002). **Some relevant aspects of the use of FTIR associated techniques in the study of surfaces and coatings**. Progress in organic coatings, **44** (3), 233-242.

49. Kumar, R. (2011). **Development and Potential Applications of Nanomaterials for Arsenic Removal from contaminated Ground water.** TRITA LWR Degree project 11:07; 17p.

50. Lamontagne, J., Dumas, P., Mouillet, V. and Kirster, J. (2001). **Comparison by Fourier Transform Infrared (FTIR) Spectroscopy of different ageing techniques: application to road bitumens.** Fuel, **80** (4), 483 - 488.

51. Li, Z., Mu,T., Jiang, T., Du, J., Zhao, G., Zhang, J., Han, B., and Huang,Y. (2004). **Tautomeric equilibrium of ethyl acetoacetate in compressed CO_2 + ethanol and CO_2 + methanol mixtures.** Spectrochimica Acta PartA, **60,** 1055-1059.

52. Miller, A. and Tanner, J. (2008). **Essentials of chemical biology: structure and dynamics of biological macromolecules.** John Wiley and Sons, LTD.

53. Bloch, D.R. (2006). **Organic chemistry demystified**. McGraw –Hill Companies, Inc.

54. Still, T. (2010). **High Frequency Acoustics in Colloid-Based Meso- and Nanostructures by Spontaneous Brillouin Light Scattering**. Springer.

55. Sivasankar, B. (2008). **Engineering Chemistry.** Tata McGraw – Hill Publishing Company Limited, 7 West Patel Nagar, New Delhi 110 008, Chapt. 10, pp 300.

CHAPTER 4

Hydrothermal processing of TiO_2 nanostructures: The effect of NaOH / NH_4OH ratio on TiO_2 nanostructures

4.1 Introduction

In this chapter, NaOH and NH_4OH were individually used for the hydrothermal processing of nanomaterials with TiO_2 P-25 Degussa. This was followed by using the co-solvent approach. This comprised the preparation of the co-solvent solution at different ratios of the base solvents. The co-solvent solution of a given ratio was reacted with the TiO_2 P-25 Degussa. The objective was to investigate the effect of different bases and ratios on the morphology of the TiO_2.

4.2 Experimental

4.2.1 Hydrothermal processing of TiO_2 nanomaterials

The hydrothermal method was carried out in an autoclave reactor at 150 °C using TiO_2 as a starting material. The synthesis was carried out by first reacting NaOH with TiO_2 P-25 Degussa. The synthesis was then carried out by reacting TiO_2 P-25 Degussa with the co-solvent approach at different ratios. A volume of 90 cm^3 of 18 M NaOH was transferred into a 1 litre beaker. A mass of 12.00 g of TiO_2 was added into the beaker. The mixture was stirred with a glass rod until a suspension was formed. The mixture was then transferred to a Teflon-lined autoclave and was heated at 150 °C for 24 hours with constant stirring (500 rpm). The mixture was then allowed to cool to room temperature. The solid product was then separated from the mixture by centrifugation at 4500 rpm for 10 minutes. The solid was washed with deionised water several times until the conductivity of the supernatant liquid was less than 100 µS /cm. The solid was eventually vacuum-dried overnight in an oven at 100 °C. The above synthesis procedure using 70 cm^3 NaOH and 20 cm^3 NH_4OH was repeated for the experiments on the four co-solvent ratio solutions. The synthesis procedure is summarized in Table 4.1.

Table 4.1 : Experiments for synthesis of TiO_2 nanomaterials

Sample	TiO_2/g	NaOH / cm^3	NH_4OH / cm^3
A1	12.0	90.00	0.0
A2	12.0	70.00	20.0
A3	12.0	45.00	45.0
A4	12.0	40.00	50.0
A5	12.0	50.00	40.0

4.2.2 Characterization of TiO_2 nanomaterials

Various characterization techniques were used. Two different scanning electron microscopes were used, the reason being that the FIB-SEM gives very good images whereas the field emission scanning electron microscope that was used for EDX does not.

4.2.2.1 X-ray diffraction (XRD)

The XRD analysis was performed to determine crystallinity of the nanomaterials using the PANalytical X' Pert Pro PW 3060/60 x-ray diffractometer. A Cu x-ray tube was used with K_α λ = 0.154 nm. The diffractometer was operating at 45.0 kV and 40.0 mA. The data was collected in the 2θ angle ranging from 1 to 90^0 with a step size of 0.02^0. Prior to analysis the sample holder was first cleaned with iso propanol to avoid contamination, and this was done for all the samples.

4.2.2.2 Scanning electron microscopy (SEM)

SEM analysis was performed to determine the morphology of the materials. The morphology was checked with a focused- ion beam (FIB - SEM) of model Auriga from Carl Zeiss. The instrument was operated at a voltage of 3.0 kV. The carbon tape was used, it was pasted on the aluminium stubs and the sample was mounted on the carbon tape, and then the stubs were placed on the SEM sample holders. Prior to SEM analysis, the samples were first carbon coated by using EMITECH K950X carbon evaporator, to make the sample surface

conductive, because the surface of TiO_2 is not conductive and that causes sample charging during this analysis.

4.2.2.3 Transmission electron microscopy (TEM)

The morphology of the nanomaterials was further determined by transmission electron microscopy (TEM) using the JEOL TEM – 2100 electron microscope. For the TEM sample preparation, the samples were suspended in ethanol, and this was followed by sonication for 10 minutes. Then the suspension was placed on a copper grid.

4.2.2.4 Energy dispersive x-ray spectroscopy (EDX)

Energy dispersive x-ray spectroscopy (EDX) was performed to determine the chemical composition of the materials. A JEOL JSM-7500F field emission scanning electron microscope was used, the sample preparation was the same as the one for the SEM analysis.

4.2.2.5 Brunauer-Emmett-Teller (BET) method

The surface areas of the nanomaterials were measured by using a Micromeritics Tristar II equipment. Prior to analysis, the samples were out- gassed in vacuum using a Vac Prep 061 Sample Degas System at 100 ^{0}C overnight, in order to remove the moisture and the volatile substances. The specific surface areas and the pore volumes of the nanomaterials were then determined by the Brunauer – Emmett- Teller (BET) method.

4.2.2.6 Fourier transform infrared spectroscopy (FTIR)

Fourier transform infrared spectroscopy (FTIR) was used to provide information about the chemical bonding present in the material and the presence of –OH groups. The model spectrum 100 FTIR spectrometer from Perkin Elmer was used.

4.3 Results

4.3.1 XRD

The XRD patterns of the starting material (P-25 Degussa TiO_2) is shown in Figure 4.1. The material consists of 80% anatase at $2\theta = 25$ ° and 20% rutile at $2\theta = 27$ °, and these peaks corresponds to (101) and (110) diffraction lines of TiO_2. Anatase TiO_2 was again observed at $2\theta = 48$ ° corresponding to (200) diffraction line, while rutile was observed at $2\theta = 36$ ° and

2θ = 55° corresponding to (004) and (211) respectively [1,2,3]. These peaks are very sharp. After reaction with 18 M NaOH, Figure 4.2 a (sample A1) the material became amorphous, and there were no peaks that could be assigned to any of the titania polymorphs. The peaks are now broad. The XRD patterns of the TiO_2 nanomaterials synthesized by the hydrothermal method using co-solvent approach, whereby NaOH and NH_4OH (samples A2-A5) were used with different ratios also shows no sharp peaks at all, the patterns do not differ much from the 100% NaOH prepared (sample A1). The material is amorphous with no definite peak formation that can be assigned to any structure.

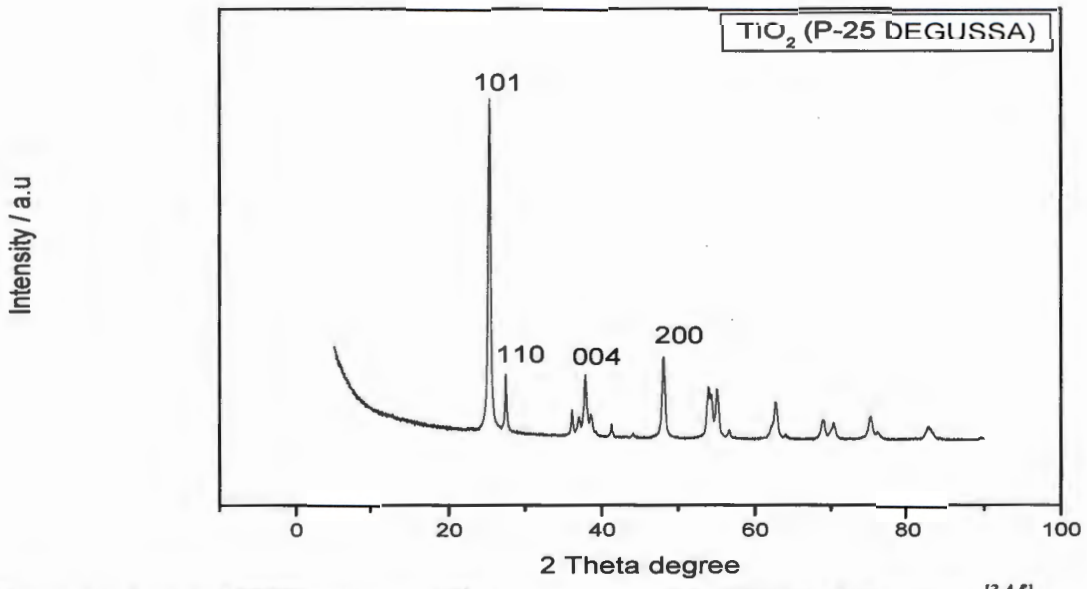

Figure 4.1: Indexed XRD patterns of the starting material (TiO_2 P-25 Degussa) [3,4,5]

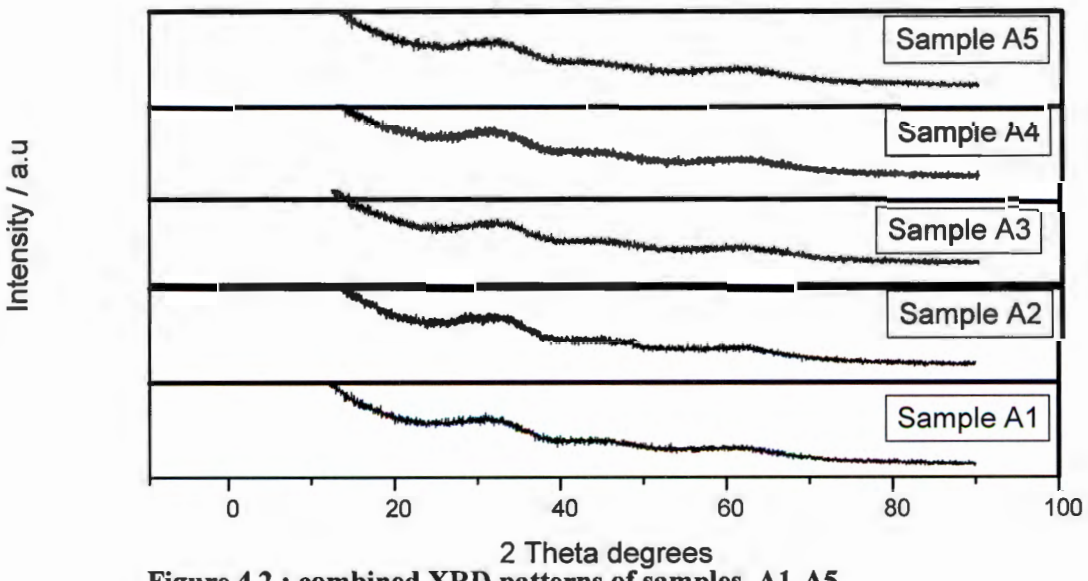

Figure 4.2 : combined XRD patterns of samples A1-A5

4.3.2 SEM images

SEM image of the starting material (P-25 Degussa TiO_2) is shown in Figure 4.3. This material consists of conglomeration of spherical clusters [1]. Figure 4.4(a) shows the SEM image of the sample treated with 18M NaOH in a 90 ml. The material is spherical in shape, but with a lot of clusters. Figure 4.4 (b-e) shows the SEM images of the materials prepared by the co-solvent approach, whereby NaOH and NH_4OH were used at the same time. Figure 4.4(b) shows the SEM image of sample A2, the material is composed of spherical clusters that is very clustered. As compared to the other five samples (Figures a-e), this one is homogenously dispersed. Figure 4.4(c) shows the SEM image of sample A3, the material is also spherical with clusters. Figure 4.4(d) shows the SEM image of sample A4, this material also consists of spherical structures. The material also consists of clustered aggregates. Figure 4.4(e) also has a spherical structure, but with a few clustered aggregates.

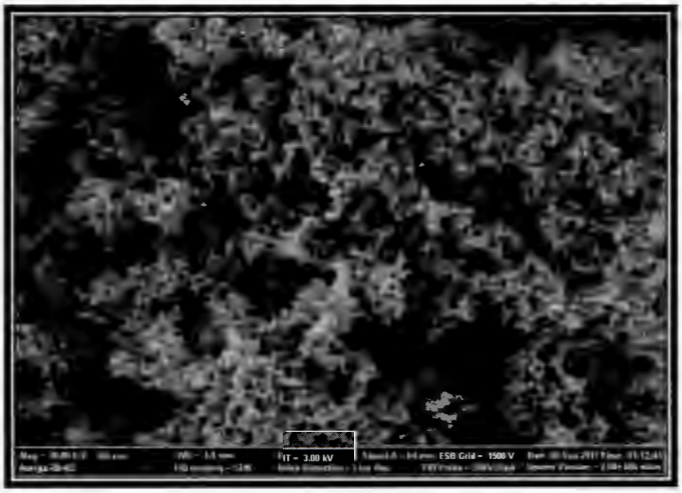

Figure 4.3: SEM image of the starting material (TiO_2 P-25 Degussa

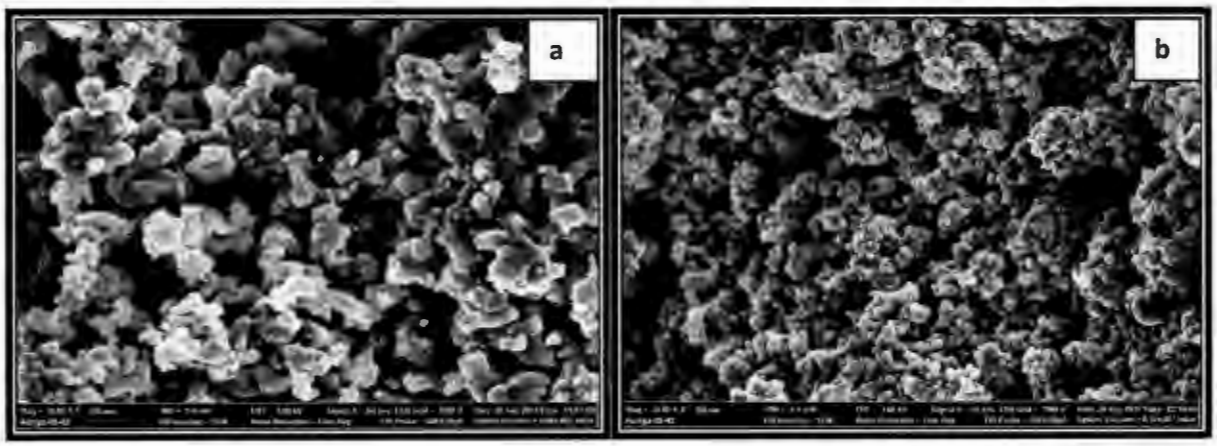

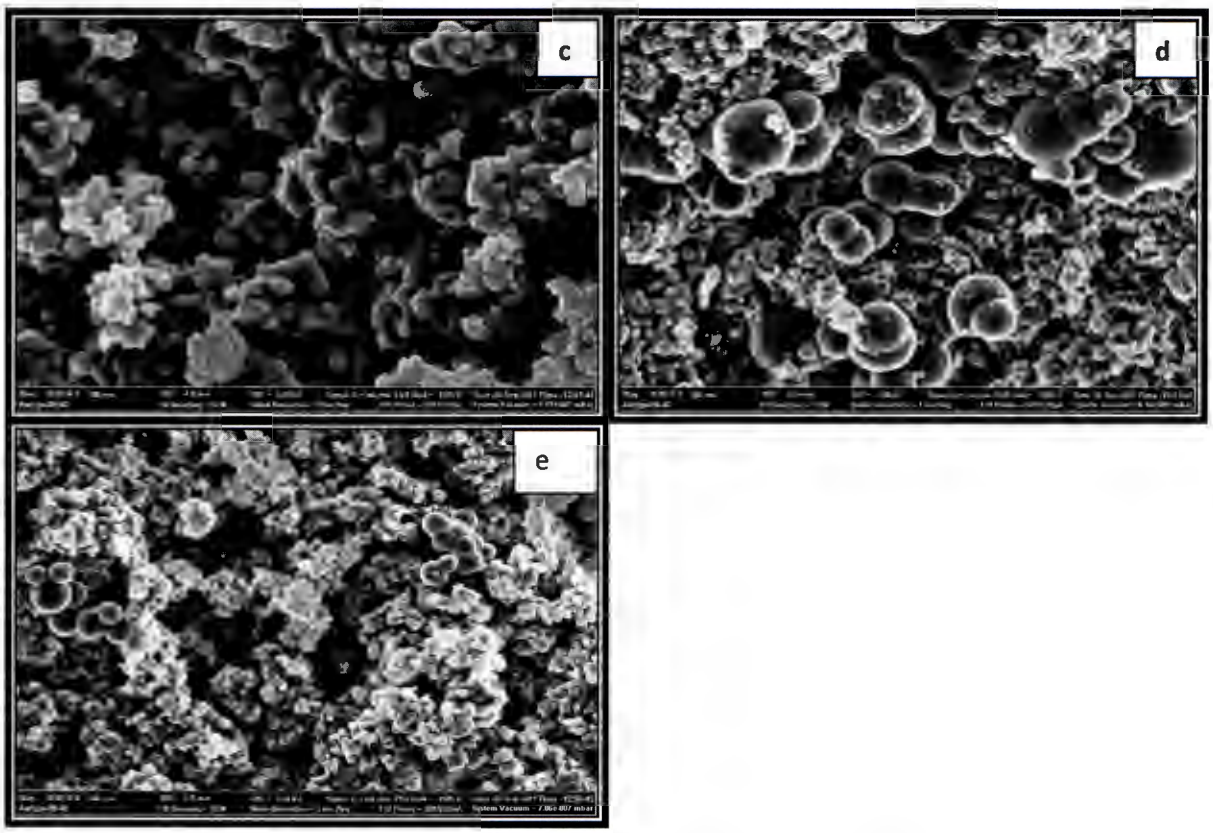

Figure 4.4: SEM images of a) sample A1 (b) sample A2 (c) sample A3 (d) sample A4 and (e) sample A5

4.3.3 TEM images

The TEM image of the starting material (P-25 Degussa) is shown in Figure 4.5. The material is spherical in shape and consists of agglomerates with an average diameter of 6-39 nm. After treatment with 18 M NaOH (Figure 4.6 a), the spherical structure was still observable but the spheres seem to have formed clustered agglomerates with an average diameter of 3-34 nm. When the co-solvent approach was introduced (NaOH and NH_4OH), Figures 4.5 (b – e), samples A2-A5, the TEM images look very similar to one another. The clusters are more agglomerated and the samples had average diameters of 3-11 nm, 11-77nm, 18-55 and 18-65 nm respectively.

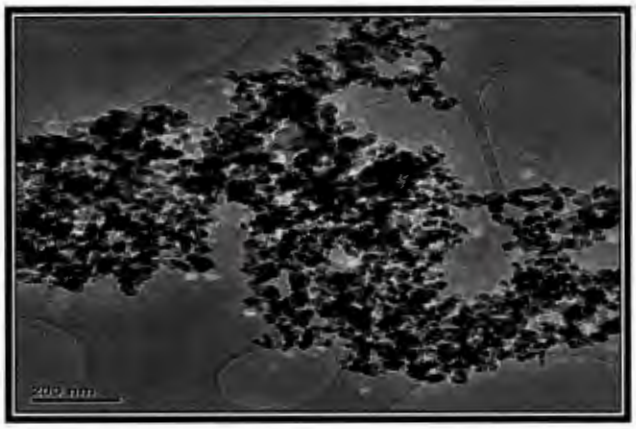

Figure 4.5 :TEM image of the starting material (P-25 Degussa TiO_2)

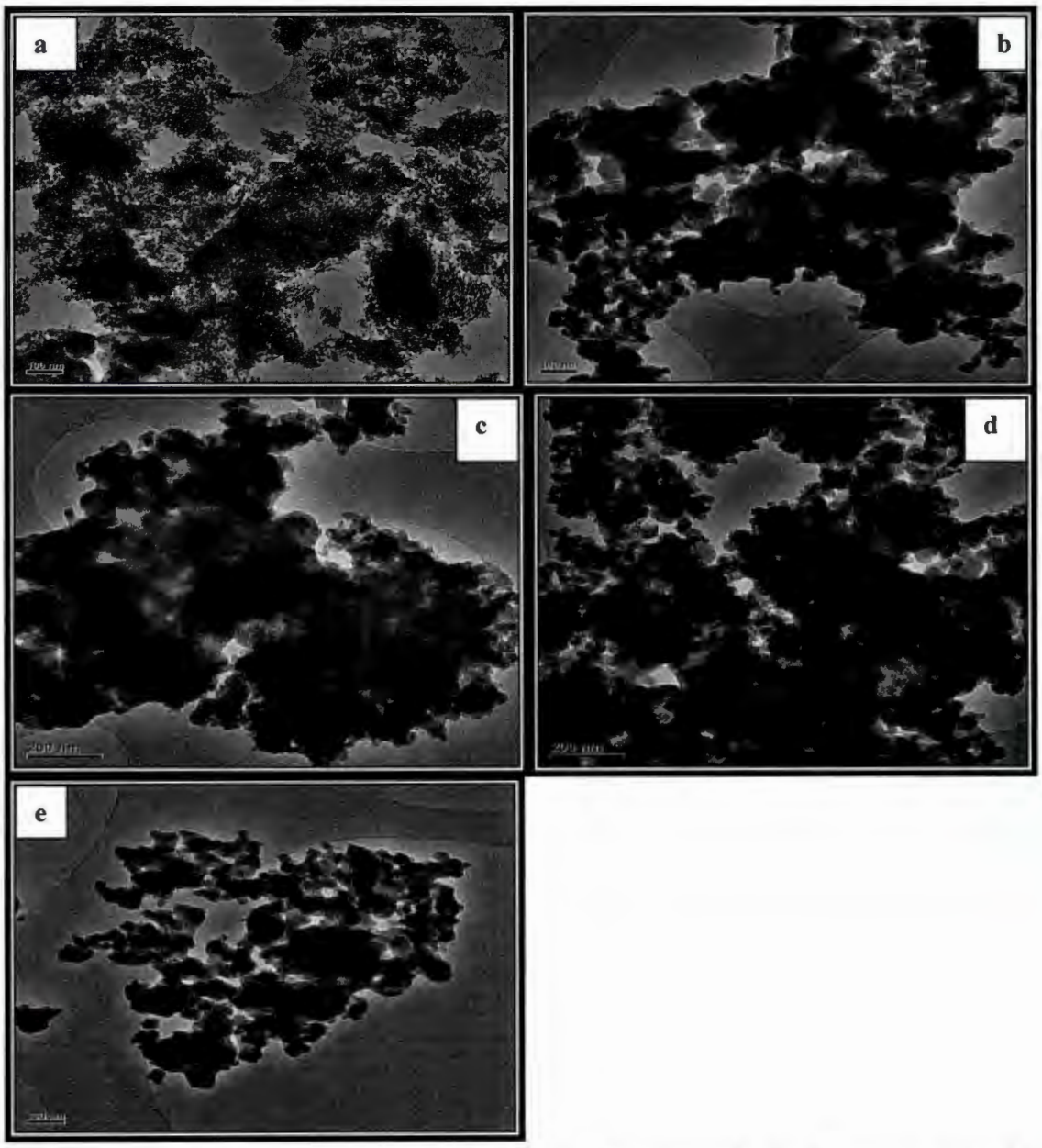

Figure 4.6:TEM images of (a) sample A1 (b) sample A2 (c) sample A3 (d) sample A4 and (e) sample A5.

4.3.4 BET surface areas

The specific surface area and the porosity of the nanomaterials were later determined by the Brunauer- Emmett-Teller method, and the results are given in Table 4.2. The specific surface area of the starting material was 47.3307 m^2 / g . After treatment with 18 M NaOH 90 cm^3, (sample A1) , the surface area increased to 60.7072 m^2/g, and then for samples A2- A5 (NH_4OH treated) the surface area decreased to 26.56 m^2/g. It was less than that of the starting material since NH_4OH was introduced as a co- solvent with varying volumes, the surface area increased with an increase in NH_4OH , the increase was ranging from 26.56 - 31.77 m^2 / g.

Table 4.2: BET surface areas

Sample name	**Surface area (m^2 / g)**
P- 25 Degussa TiO_2	47.3307
Sample A1	60.7072
Sample A2	26.5685
Sample A3	27.4066
Sample A4	25.7020
Sample A5	31.7701

4.3.5 FTIR spectroscopy

FTIR spectroscopy was used to determine the –OH groups that may be present in the samples. In Figure 4.7, all the samples (A1 – A5) have a strong O-H stretching vibration observed between 3600-2500 cm^{-1} . A peak is observed at around 1625 cm^{-1} which is due to the O–H bending in the material. And all the samples A1 – A5, have a broad peak from 3617 – 3023 cm^{-1} , which is due to the -OH stretching vibrations of surface hydroxyl groups. The two -OH stretch vibrations observed suggest the presence of different chemical enviroments of the hydroxyl groups in the material [4]. The Ti - O bonds were also observed at 600 - 500 cm^{-1} [5,6].

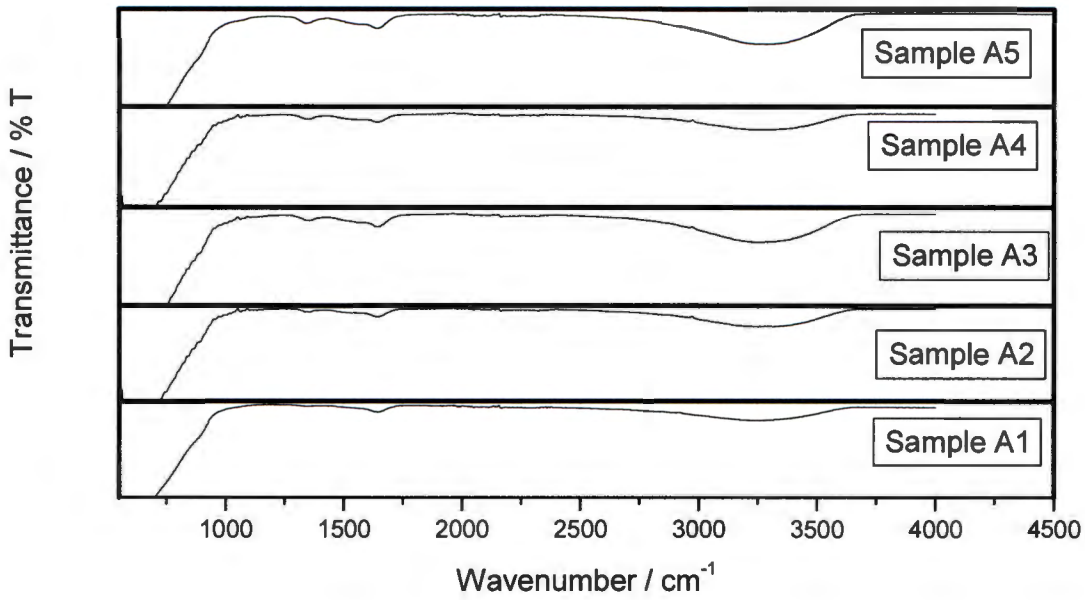

Figure 4.7: FTIR spectra of samples A1 – A5

4.4 Discussion

The XRD patterns for the starting material have sharp peaks due to the crystallinity of the material. The XRD is indexed according to the JSPD file from the article[4,5]. Sample A1 does not have any peaks that can be assigned to the titania polymorphs. Instead, the patterns have broad peaks that are due to smaller particle sizes decreasing at structural transformation. The XRD patterns for the samples treated with the co-solvent approach (NaOH and NH_4OH) were found to be identical to the one for 100 % NaOH, and this shows that NH_4OH has no influence on the structure of the material [6].

The SEM images of sample A1 show that the morphology was not transformed, it is similar to the one for TiO_2 P-25 Degussa (starting material). And this can be due to the concentration of 18 M NaOH that was used. It has been shown that a concentration of a base has an influence on the morphology of the materials [5,6]. The images of samples A2 – A5 also show that the morphology was still spherical with a lot of clusters and aggregates. This shows that NH_4OH does not influence the morphology transformation of the nanomaterials. This is because it is a weak base [6]. NH_4OH only influenced the formation of clustered aggregates.

The TEM image of sample A1 shows that the diameter has decreased from 6 – 39 nm to 3 – 11 nm. This can be attributed to the structural transformation. The images for the samples

treated by the co-solvent approach (samples A2 – A5) show that the average diameters have increased, they are greater than the one for the starting material. This is due to the formation of clusters.

The increase in the surface area of sample A1 can be attributed to the structural transformation of the material. Because the morphology was not transformed but the surface area increased, and this shows that the surface area does not only depend on the morphology transformation but also on the structural transformation. The surface areas of samples A2 – A5 decreased. This is because NH_4OH is a weak base, and it does not affect the crystal structure of TiO_2. The low surface area can also be attributed to the presence of amorphous material.

The –OH groups observed from FTIR is from the water obtained from moisture in the environment and the water that was used in the experiment.

4.5 Conclusion

The nanomaterials were successfully prepared by the hydrothermal method, using TiO_2 P-25 Degussa which is a commercially available TiO_2 and 18 M NaOH. The morphology of the nanomaterials was similar to that of the starting material (TiO_2). The hydrothermal processing of TiO_2 with NaOH has previously been done and nanotubular materials have been obtained [5]. But NaOH is known to transform the morphology of TiO_2 P-25 Degussa when it is in the concentration of 10 M. But in this study, a concentration of 18 M was used, and it was observed that this concentration does not transform the spherical morphology of the starting material (P -25 Degussa TiO_2). For this sample the surface area increased a bit but the morphology did not, this is due to the structural transformation. And this shows that the concentration of a base has an influence on the morphology of the nanomaterials. Even the nanomaterials prepared by co-solvent approach (NH_4OH and NaOH), they have a morphology similar to that of the starting material. This shows that NH_4OH has no influence in the morphology of TiO_2 nanostructures when it is used together with 18 M NaOH since it is a weak base. The XRD results show that NH_4OH has no influence on the microstructure on the materials.

4.6 References

1. Ohno, T., Sarukawa, K., Tokieda, K. And Matsumura, M. (2001). **Morphology of a TiO_2 Photocatalyst (Degussa, P-25) consisting of Anatase and Rutile Crystalline Phases.** Journal of Catalysis, **203**, 82-86.

2. Primo, A., Corma, A., and Garcia, H. (2010). **Titania supported gold nanoparticles as photocatalyst**. Institution de Tecnologia Quimica , Universidad Politecnica de Valencia-CSIC, Camino de Vera,46022 Valencia, Spain.

3. Thamaphat, K., Limsuwan, P. and Ngotawornchai, B. (2008). **Phase Characterization of TiO_2 Powder by XRD and TEM.** Kasetsart J. (Nat. Sci), **42**, 357-361.

4. Wang, X., Liu, G., Wang, L., Pan, J., Lu, G.Q and Cheng, H.-M. (2011). **TiO_2 films with oriented anatase {001} facets and their photoelectrochemical behavior as CdS nanoparticle sensitized photoanodes.** J. Mater. Chem., **21**, 869-873.

5. Watson, S., Beydoun, D., Scott, J. and Amal, R. (2004). **Preparation of nanosized crystalline TiO_2 particles at low temperature for photocatalysis**. Journal of Nanoparticle Research, **6**, 193-207.
6. Sikhwivhilu, L.M, Sinha Ray, S, and Coville, N.J.,(2009).**Influence of bases on hydrothermal synthesis of titanate nanostructures**. Applied Physics A Materials Science and Processing, **94**, 963-973.

7. Beranek, R. and Kisch, H. **Tuning the Optical and Photoelectrochemical Properties of Surface-Modified TiO_2.** Institut für Anorganische chemie der Universitat Erlangen- Nürnberg, Ergerlandstr. 1, D-91058, Erlangen Germany.
8. Variola, F., Nanci, A.and Rosei, F.(2009). **Assessment of the Titanium Dioxide Absorption Coefficient by Grazing-Angle Fourier Transform Infrared and Ellipsometric Measurements**. Society for Applied Spectroscopy, **63** (10), 1187-1190.
9. Wong, C.L., Tan, Y.N., and Mohammed, A.R. (2011). **A review on the formation of titania nanotube photocatalyst by hydrothermal method**. Journal of Environmental Management, **92**, 1669-1680.

10. Peng, Y., Kansal, S.K. and Deng, W. (2009). **Studies on transformation of titanate nanotubes into nanoribbons.** Materials Letters, **63**, 2615-2618.

CHAPTER 5

Hydrothermal processing of TiO_2 nanostructures :The effect of KOH/ NaOH mole ratio on the TiO_2 nanostructures

5.1 Introduction

This chapter is a study of the effect of the various KOH / NaOH mole ratios on the morphology of TiO_2 P-25 Degussa. Section 5.2.1 describes the experiments that were conducted for the synthesis of TiO_2 nanostructures. Section 5.2.2 outlines the characterization of the products from the preceeding section. Section 5.3 presents the results that were obtained. Finally, sections 5.4, 5.5 and 5.6 give respectively the discussion, conclusion and references.

5.2 Experimental

5.2.1 Synthesis of TiO_2

The hydrothermal method was used here for the synthesis of the TiO_2 nanostructures. The mole ratios of KOH to NaOH were prepared: 50 % KOH / 50 % NaOH ; 30 % KOH / 70% NaOH ; 10 % KOH / 90 % NaOH. The three samples were then named B1, B2 and B3 respectively. A 90 cm^3 solution of each mole ratio was transferred into a 1 litre beaker to which 12.00 g of TiO_2 (P-25 Degussa) was added. The procedure outlined in chapter 4, section 4.2.1 was followed. A summary of the procedure is given in Table 5.1.

Table 5.1: Synthesis of TiO_2 by treatment with NaOH and KOH

Sample designation	NaOH	NaOH	KOH	KOH	TiO_2 / g
	G	% mol	g	% mol	
B1	32.4	50.00	32.4	50.00	12.00
B2	28.8	44.00	36.0	56.00	12.00
B3	25.9	40.00	38.9	60.00	12.00

5.2.2 Characterization of TiO_2

The TiO_2 nanostructures that were obtained were characterized according to the procedure outlined in chapter 4, section 4.2.2.

5.3 Results

5.3.1 XRD patterns

The XRD patterns of samples B1 – B3 are shown in Figure 5.1. For sample B1 , there are peaks observable at $2\theta = 25^0$ and at $2\theta = 27^0$ which are the characteristic peaks of anatase and rutile TiO_2, respectively and these peaks corresponds to (101) and (110) diffraction lines of TiO_2. A peak observed at $2\theta = 48^0$, indicates anatase and it corresponds to (200) diffraction line [1].There is also a peak that is observed at $2\theta = 10^0$ which can be assigned to the titanate structure [2]. Because of the presence of peaks we can deduce that this material is crystalline. For sample B2, the same peaks were also observed, but they were less intense and unresolved. This material has very little crystallinity than sample B1. No diffraction peaks were observed for sample B3. this material was found to be amorphous. As the amount of KOH was decreased, the crystallinity decreased. KOH played a huge role in the crystallinity and the morphology transformation of the materials.

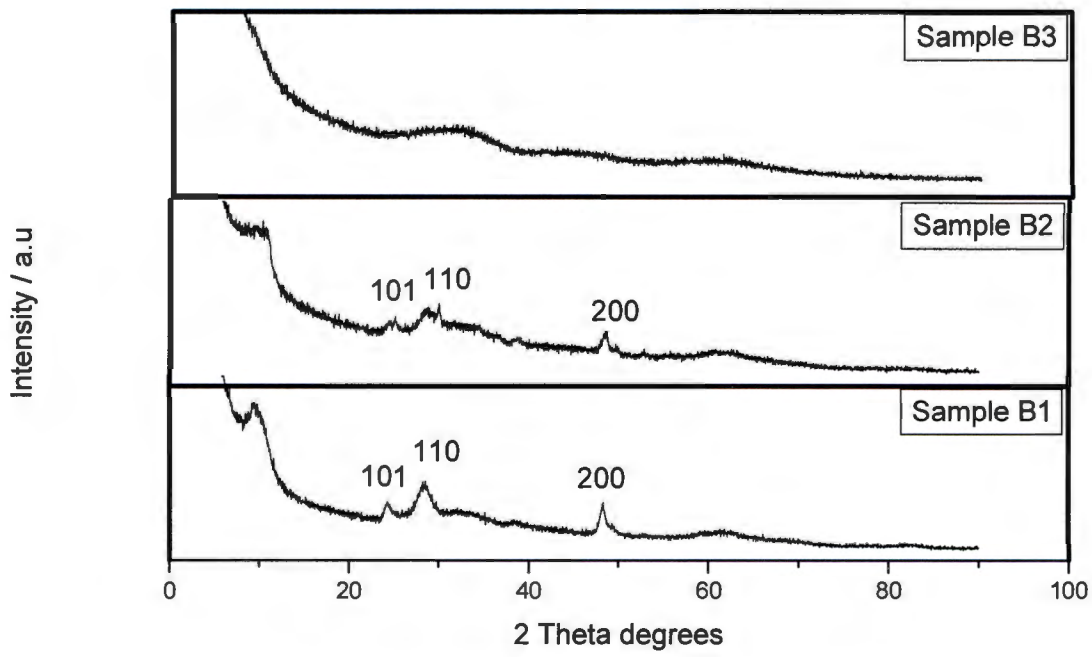

Figure 5.1: Indexed XRD patterns of samples B1- B3 [1,3]

5.3.2 SEM images

The SEM images are shown in Figure 5.2 (samples B1 – B3). Sample B1 consists of more nanotubes and nanorods than TiO_2 clusters. Morphology transformation in sample B2 was marked by the presence of nanotubes, nanobelts and TiO_2 clusters. However , they were in a small proportion. Morphology transformation decreased with the amount of KOH. Figure 5.2 c (sample B3) does not have nanobelts and nanorods. The SEM micrograph indicates that the material has spherical structures. Morphology transformation of the TiO_2 P-25 Degussa was insignificant as there are more unreacted materials that are amorphous.

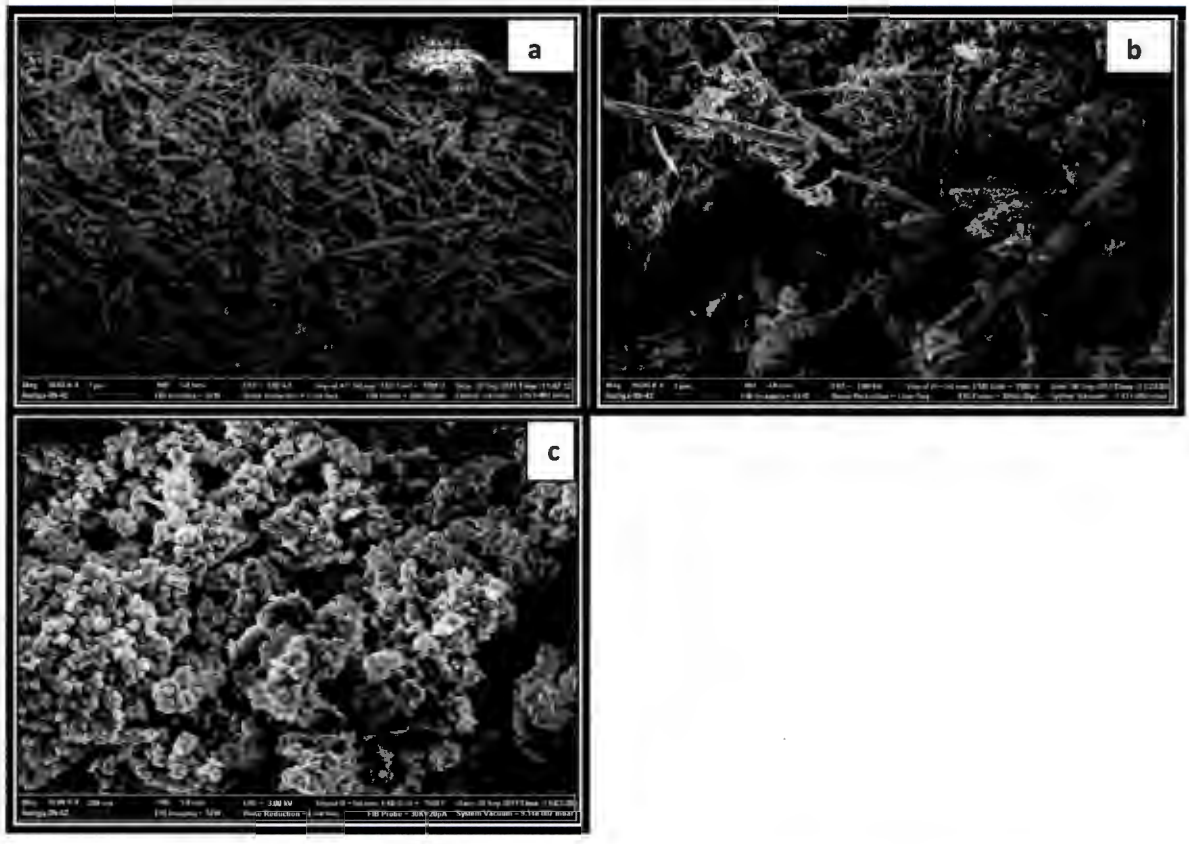

Figure 5.2: SEM images of (a) sample B1 (b) sample B2 and (c) sample B3

5.3.3 :TEM images

TEM images are shown in Figure 5.3 (samples B1- B3). Sample B1 shows the presence of nanotubes and nanorods which are randomly distributed and thin- walled, with an average diameter of 4 - 11 nm. Sample B2 comprises bundles of nanorods and nanobelts with an average diameter of 3 -18 nm. There is still some unreacted material. The TEM image of sample B3 indicates that there was no morphology transformation on the TiO_2 P-25 Degussa,

this means that the nanomaterials still retained the spherical structure. This sample has an average diameter of 8 - 20 nm.

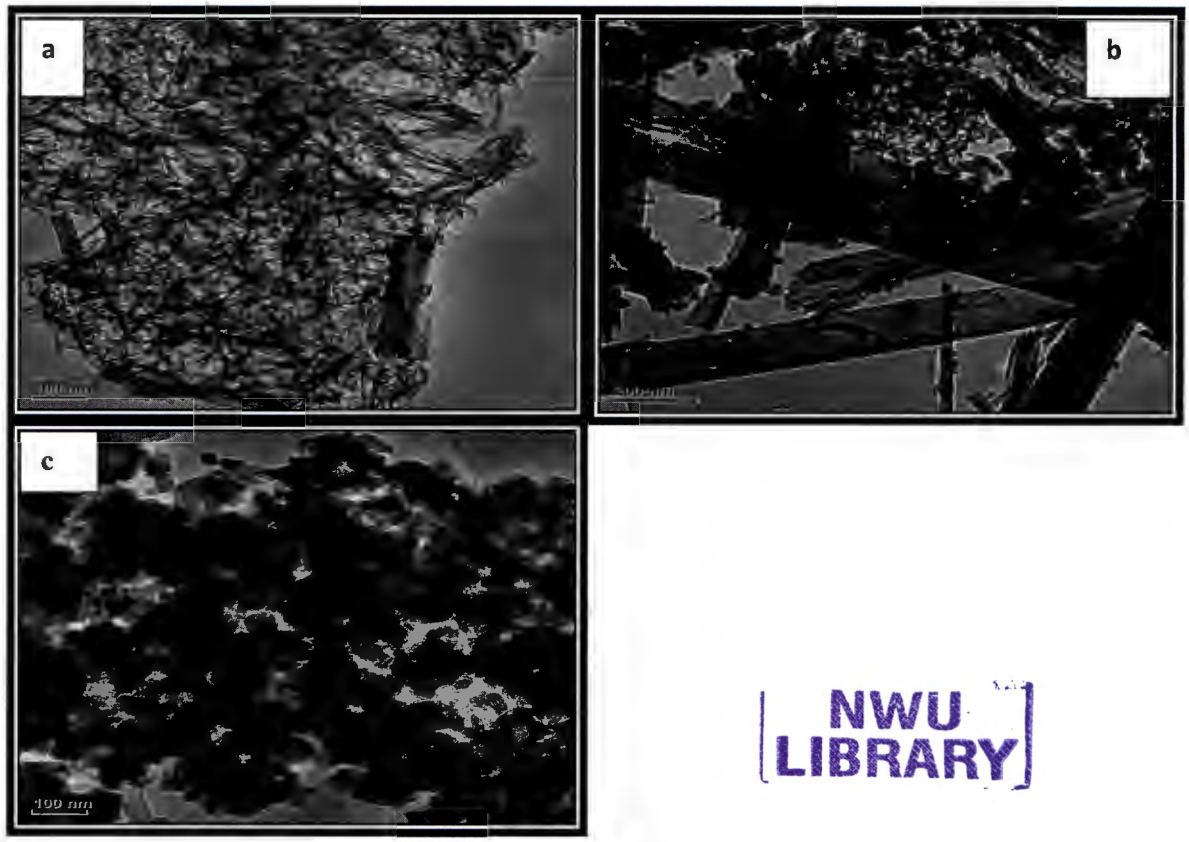

Figure 5.3 :TEM images of (a) sample B1 (b) sample B2 and (c) sample B3

5.3.4 BET results

The BET results are summarized in Table 5.2. The surface area of the starting material was 47.3 m^2 / g. The surface area increased to 134.09 m^2 / g after treatment of TiO_2 P-25 Degussa with 50 % KOH / 50 % NaOH solution. The surface area of B2, the product of the reaction of 30 % KOH / 70 % NaOH solution with TiO_2 P-25 Degussa, increased to 65.59 m^2 / g. The surface area of B3, the product of the reaction of 30 % KOH / 70 % NaOH was found to be 30.8337 m^2 / g.

Table 5.2 : BET surface areas

Sample name	Surface area (m^2 / g)
TiO_2 (P -25 Degussa)	47.3307
Sample B1	134.0964
Sample B2	65.5968
Sample B3	30.8337

5.3.5 FTIR spectroscopy

FTIR spectra are illustrated in Figure 5.4 (B1 –B3). All the samples have a strong O-H stretching vibration between 3600-2500 cm^{-1} . A peak is observed at around 1625 cm^{-1} which is due to the O–H bending in the material. And all the samples B1 – B3, have a broad peak from 3617 – 3023 cm^{-1} , which is due to the -OH stretching vibrations of surface hydroxyl groups [4]. The Ti - O bonds were also observed at 600 - 500 cm^{-1} [5,6].

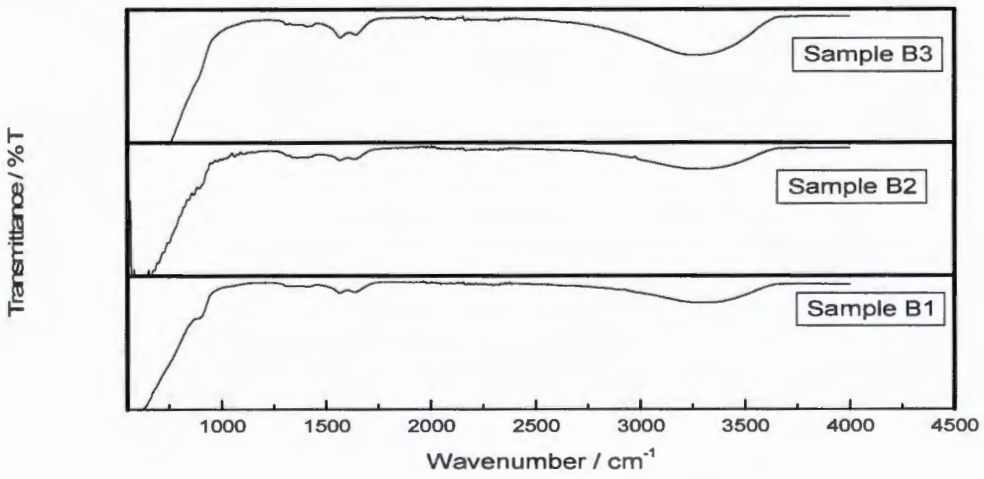

Figure 5.4: FTIR spectra of B1- B3

5.4 Discussion

The peaks observed in sample B1 show that there is anatase and rutile and there is also structural transformation, which is marked by the presence of a titanate structure. KOH played a huge role in the morphology transformation of the nanomaterials. The little crstallinity observed in sample B2 could be attributed to the decrease in the amount of KOH that was added. Sample B3 showed no diffraction peaks that could be assigned to any of the titania polymorphs. Instead there were broad peaks present and they can be due to the structural transformation. This material is amorphous.

The SEM images of sample B1 show that the morphology was transformed. This morphology transformation is because of KOH. Sample B2 showed the presence of nanowires and nanobelts but the yield had decreased. This is because the amount of KOH was decreased. Sample B3 did not show any morphology transformation, and that is due to the small amount of KOH that was used.

The TEM images show that the diameters of all the three samples (B1 – B3) have decreased, and this is due to the structural and morphological transformation. Sample B3 did not change morphology but the diameter also decreased. The decrease is attributed to the structural transformation [7].

The increase in surface areas of samples B1 and B2 is due to the morphological and structural transformation. The decrease in surface area of sample B3 is due to the amorphous material present [4].

The –OH groups observed from FTIR is from the water obtained from moisture in the environment and the water that was used in the experiment.

5.5 Conclusion

The nanomaterials were successfully prepared by the hydrothermal method using TiO_2 P -25 Degussa and KOH and NaOH with different mole ratios (samples B1 - B3). The morphology transformation was found to be dependent on the amount of KOH since it is a stronger base than NaOH . Morphology transformation increased with the amount of KOH. KOH reacts better with P -25 Degussa than NaOH. Variation of the amount of KOH led to different morphologies such as nanorods and nanobelts.

5.6 References

1. Thamaphat, K., Limsuwan, P. and Ngotawornchai, B. (2008). **Phase Characterization of TiO_2 Powder by XRD and TEM.** Kasetsart J. (Nat. Sci), **42**, 357-361.

2. Sikhwivhilu, L.M., Mpelane, S.,Moloto, N. and Sinha Ray, S. **Hydrothermal synthesis of TiO_2 nanotubes: microwave heating versus conventional heating.**

3. Sikhwivhilu, L.M., Mpelane, S, Mwakikunga, B.W. and Sinha Ray, S. (2012). **Photoluminescence and Hydrogen Gas – Sensing properties of Titanium Dioxide Nanostructures Synthesized by Hydrothermal Treatments.** Applied Materials & Interfaces, **4**, 1656 - 1665.

4. Sikhwivhilu, L.M, Sinha Ray, S, and Coville, N.J.,(2009).**Influence of bases on hydrothermal synthesis of titanate nanostructures**. Applied Physics A Materials Science and Processing, **94**, 963-973.

5. Beranek, R. and Kisch, H. **Tuning the Optical and Photoelectrochemical Properties of Surface-Modified TiO_2.** Institut für Anorganische chemie der Universitat Erlangen- Nürnberg, Ergerlandstr. 1, D-91058, Erlangen Germany.

6. Variola, F., Nanci, A.and Rosei, F.(2009). **Assessment of the Titanium Dioxide Absorption Coefficient by Grazing-Angle Fourier Transform Infrared and Ellipsometric Measurements**. Society for Applied Spectroscopy, **63** (10), 1187-1190.

7. Joshi, S.K. and Mashelkar, R.A. (1995). **Solid State Chemistry**. World Scientific Series in 20^{th} Century Chemistry, Vol. 4, pp 215.

CHAPTER 6

The effect of calcination on the TiO_2 nanomaterials treated with NH_4OH/ NaOH solutions.

6.1 Introduction

Chapter 6 investigates the effect of calcinations on the TiO_2 nanomaterials that were treated with various solutions of NH_4OH / NaOH. Section 6.2 outlines how the five samples (A1 to A5) were calcined and the various characterization techniques that were used. The next section gives the results. Sections 6.3.1, 6.3.2, 6.3.3, 6.3.4 and 6.3.5 describe the XRD patterns, SEM images, TEM images, EDX plots and BET data. Lastly, sections 6.4, 6.5 and 6.6 give the discussion, conclusion and references.

6.2 Experimental

6.2.1 The calcination of the nanomaterials

The TiO_2 nanomaterials that were calcined are given in chapter 4, Table 4.1 (samples A1 to A5). The TiO_2 P-25 Degussa was initially reacted with 90 cm^3 of 18M NaOH. The TiO_2 P-25 Degussa was subsequently reacted with the co-solvent solutions (NH_4OH / NaOH) at different ratios. The powdered TiO_2 nanomaterial products were calcined in crucibles in a Lenton BCF 13/ 12-2416 CG furnace (supplied by Elite Thermal Systems) at 300 °C for 4 hours.

6.2.2 Characterization of the nanomaterials

The calcined nanomaterials were characterized according to the procedure outlined in chapter 4, section 4.2.2.

6.3 Results

6.3.1 XRD patterns

The XRD patterns of the samples are shown in Figure 6.1. After calcining the samples at 300 °C for 4 hours, the material still remained amorphous. Samples A1, A2, A3 and A5 are amorphous and they have no definite peak that can be assigned to any of the titania polymorphs (anatase, rutile and brookite). Instead these four samples have broad peaks that

can be attributed to the structural transformation (presence of a titanate structure) [1]. Sample A4 has a peak at 2θ = 10° and it can be attributed to the titanate structure and there are also very small peaks at 2θ = 25° and 2θ = 27° and they can be assigned to anatase and rutile respectively[], but these peaks are small due to the amorphicity of the material.

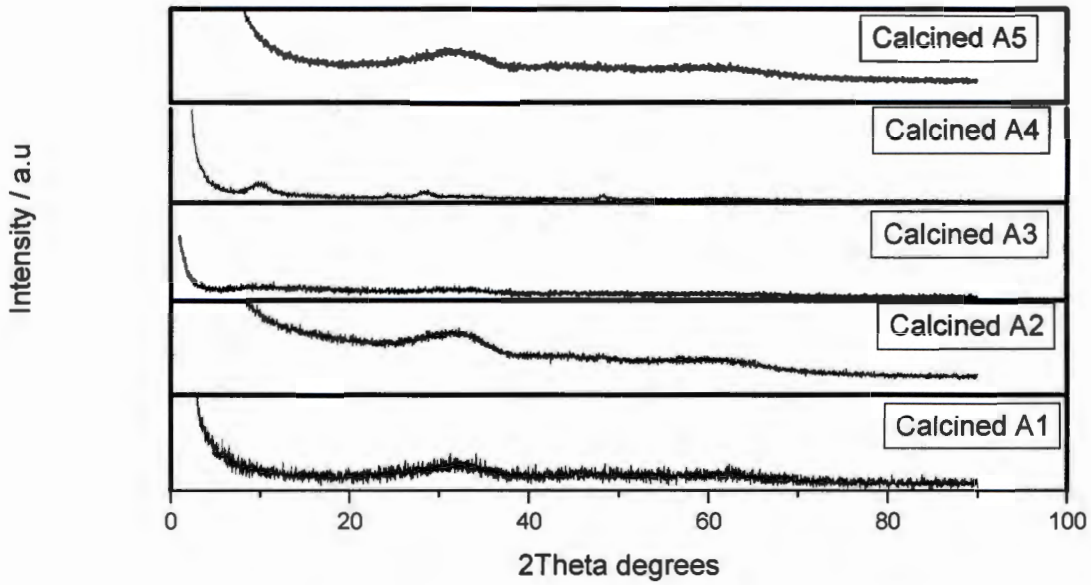

Figure 6.1: XRD patterns of the calcined Samples A1-A5

6.3.2 SEM images

The SEM images of the samples are shown in Figure 6.2. For Sample A1, after calcination the particles were still spherical and clustered. Morphology was not transformed, instead the material is agglomerated. Sample A2 is also agglomerated and it consists of clustered spherical particles and funny material which resembles nanorods and the tubular structure. Samples A3 – A5 have a similar morphology that consists of clustered spherical aggregates which are also very agglomerated. For all the samples, although the calcination temperature is low it somehow influenced the material because no unreacted material was observed.

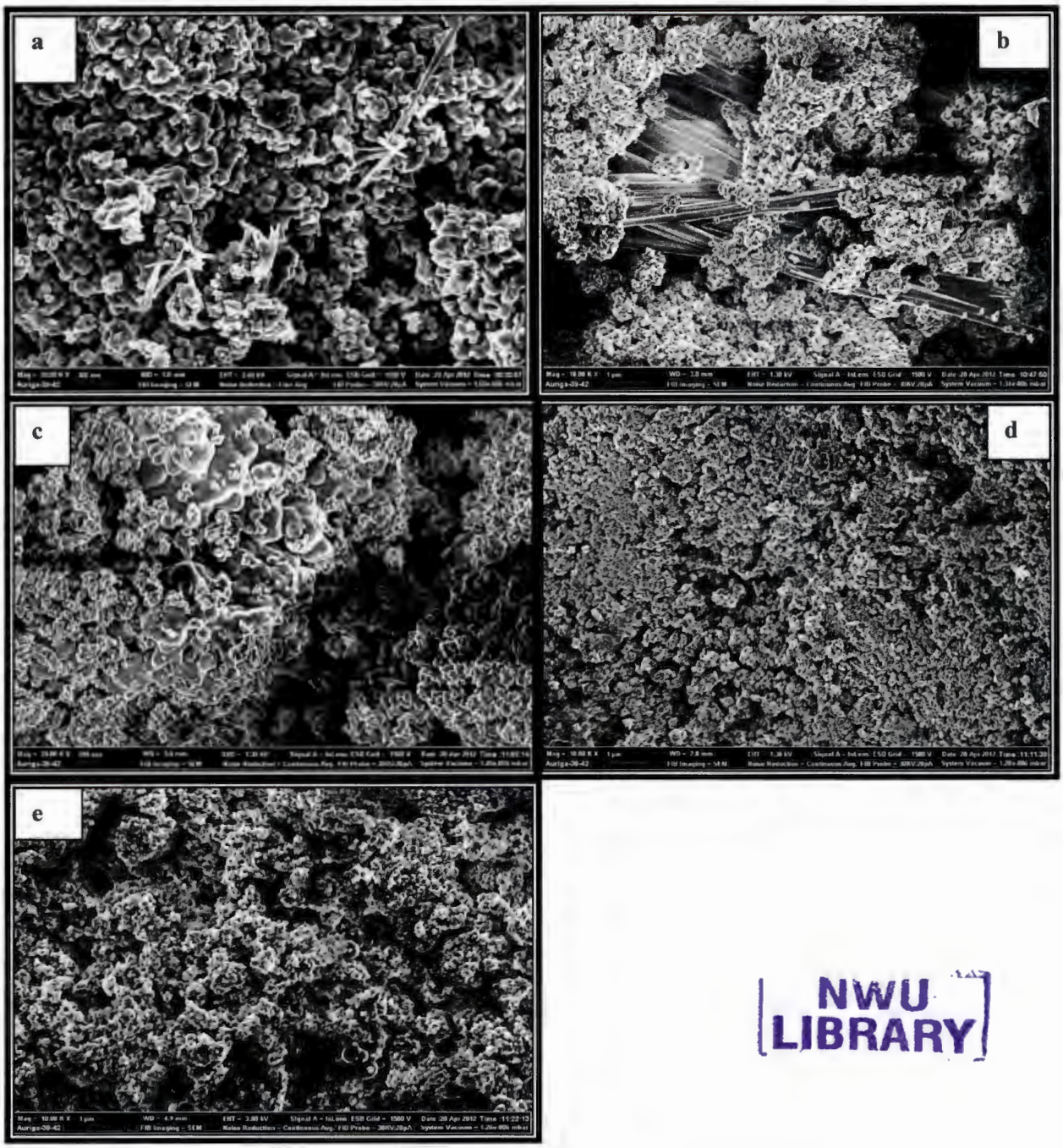

Figure 6.2 : SEM images of the calcined samples A1-A5 (a – e)

6.3.3 TEM images

The TEM images of the samples are shown in Figure 6.3. For sample A1, the material consists of spherical clusters with an average diameter of 7 - 195 nm. Sample A2 also has clustered spherical particles and material that resemble nanorods and nanotubes. The average diameter is 69 – 277 nm. Sample A3 has clustered spherical aggregates with an average diameter of 70 – 100 nm. Samples A4 and A5 also consist of clustered spherical aggregates

with average diameters of 64 – 170 nm and 69 – 250 nm respectively. The TEM images of all these samples (A1 – A5) shows that the material is agglomerated.

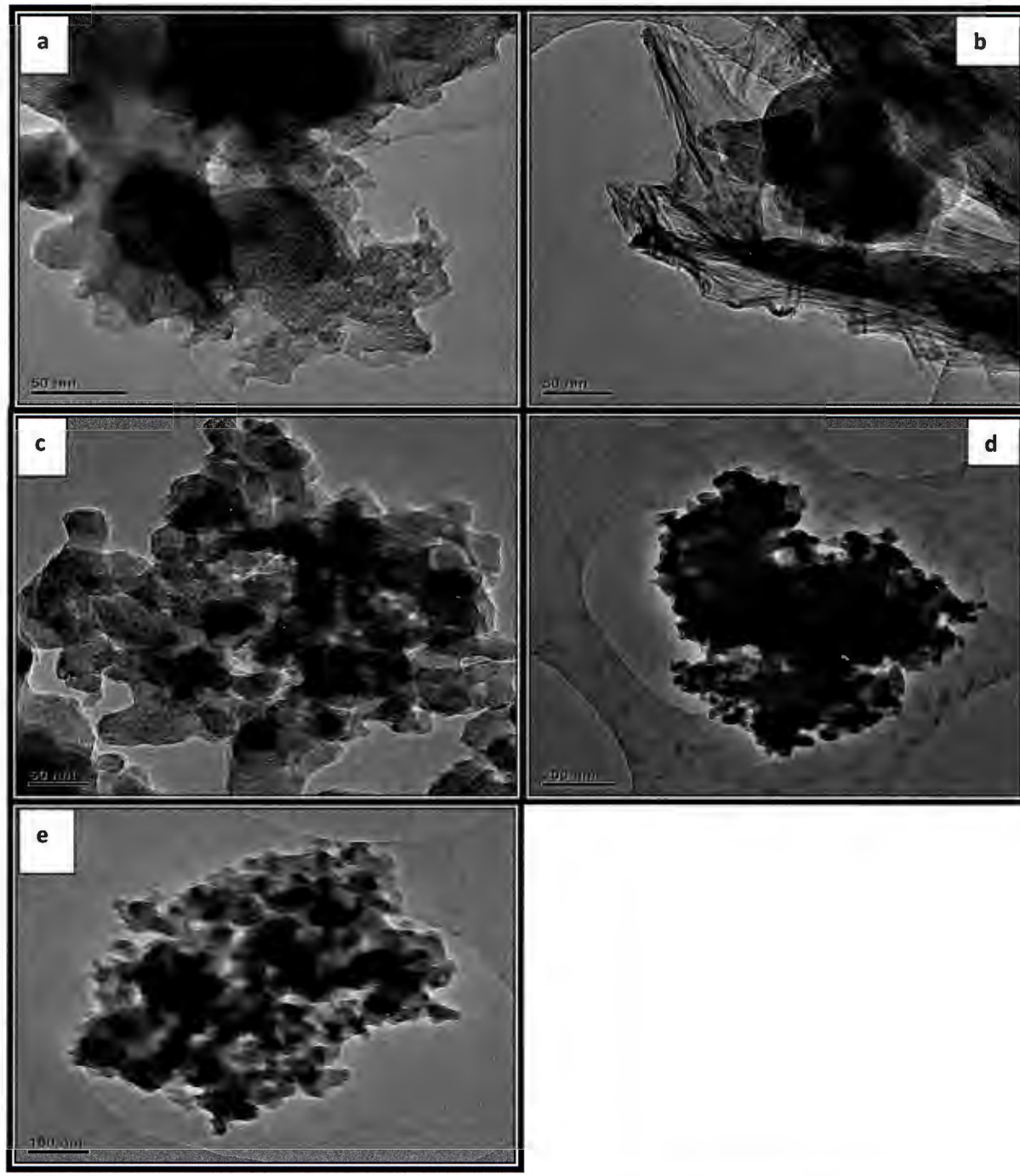

Figure 6.3 : TEM images of the calcined samples A1-A5 (a - e)

6.3.4 EDX analysis

EDX of the samples is illustrated in Figure 6.4, plots a-e. All the samples are composed of Ti, Na and O – Ti overlap. And for all the samples treated with NH_4OH, there is N that is observed but it is just an overlap. From the EDX we can deduce that the materials prepared are made up of a titanate structure of the formula $Na_2Ti_2O_4$. The EDX of the of the samples also consists of small amounts of Fe.

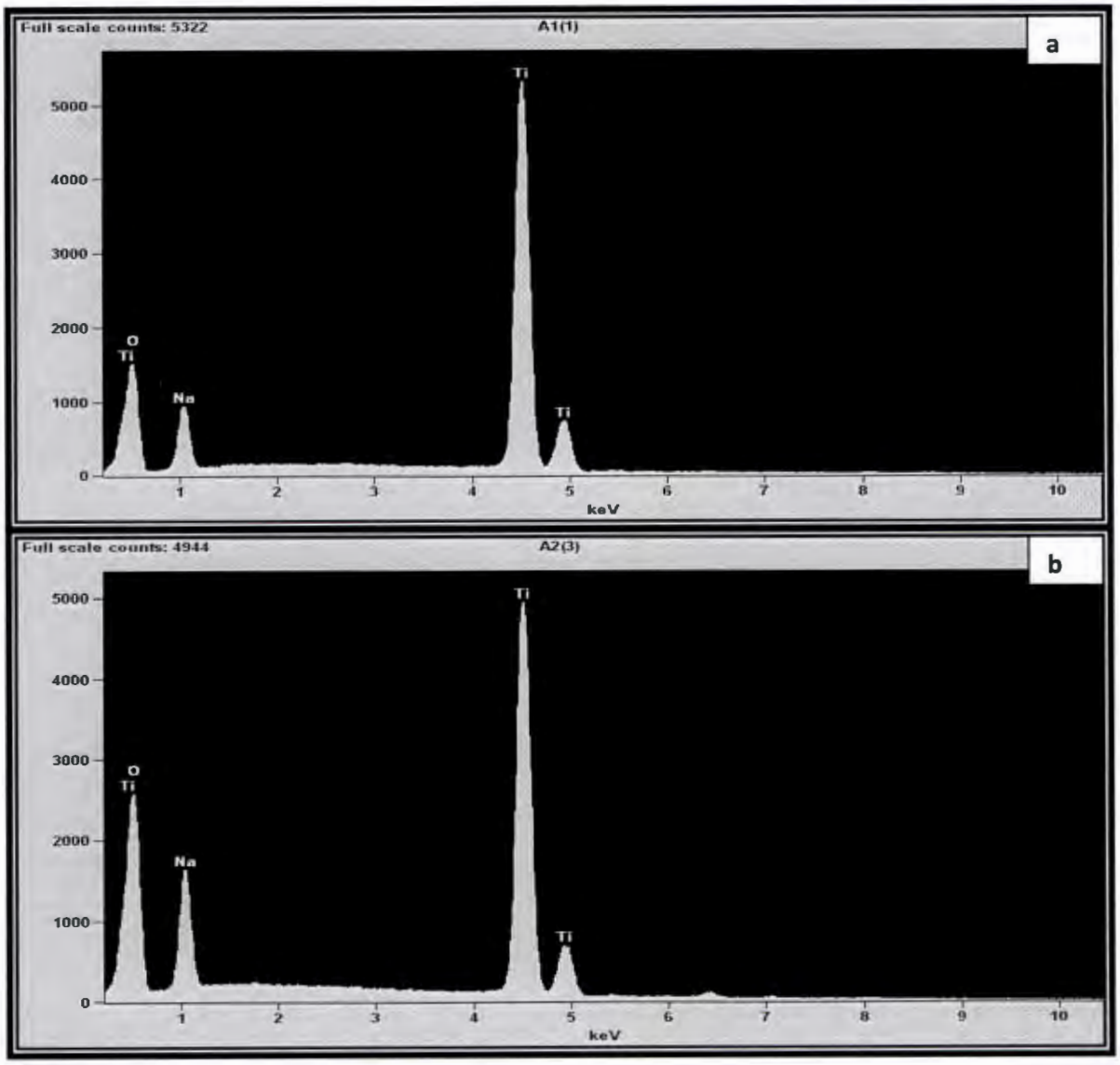

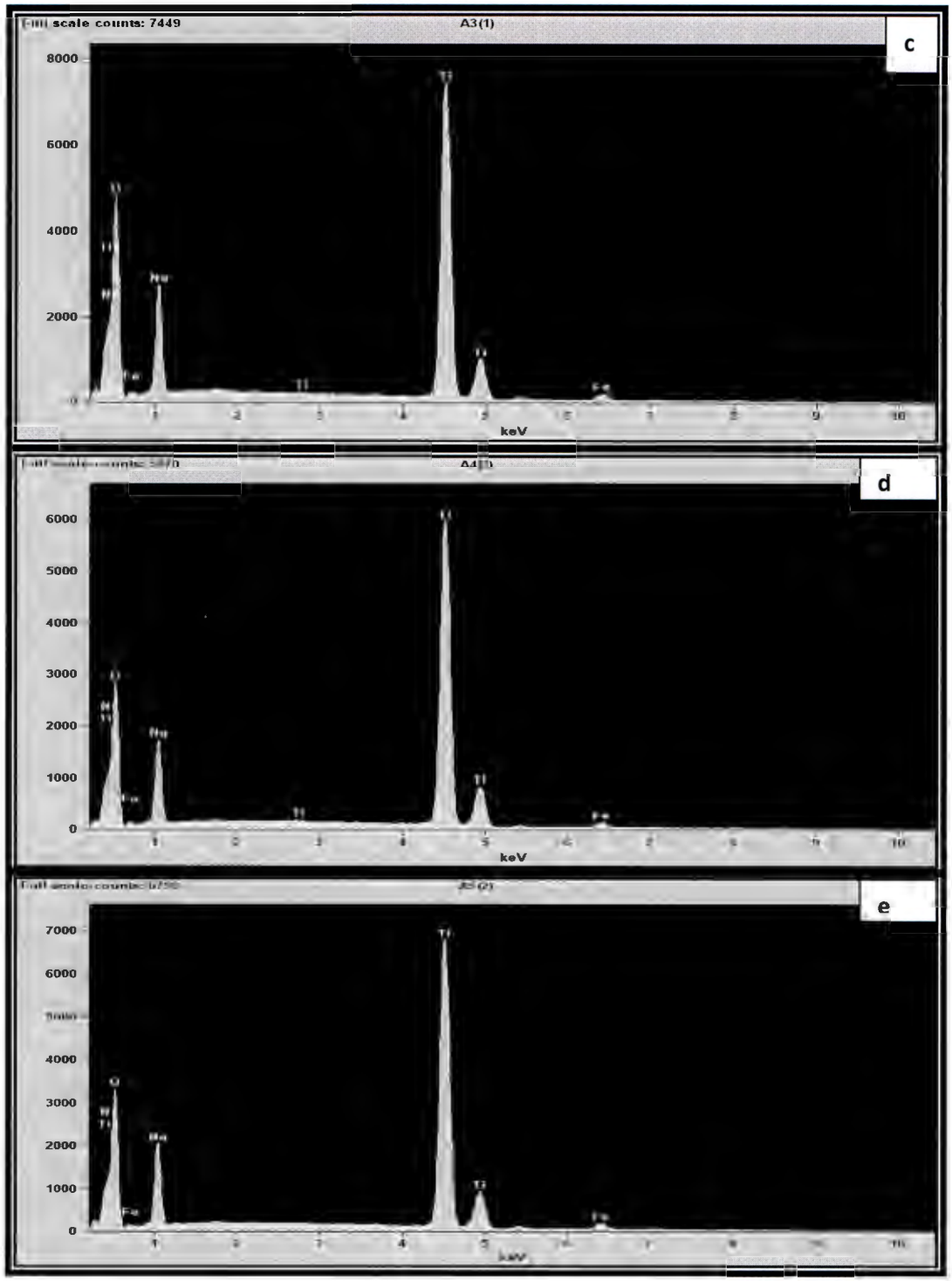

Figure 6.4 : EDX of the calcined samples A1-A5 (a - e)

6.3.5 BET results

The BET results are shown in Table 6.1. After calcination of the materials, the surface areas of all the samples (A1-A5) decreased tremendously.

Table 6.1 BET surface areas

Sample name	Surface area (m^2 / g)
Calcined Sample A1	18.6454
Calcined Sample A2	26.3780
Calcined Sample A3	23.6929
Calcined Sample A4	25.7020
Calcined Sample A5	23.4043

6.4 Discussion

The XRD patterns (section 6.3.1), there was no peak that could be assigned to any structures of the titania polymorphs. The material still remained amorphous, this could be due to the low calcination temperature of 300 °C. Most researchers have proved that the crystallinity of the nanomaterials increases with the calcination temperature. A good crystallinity has been achieved before when the temperature of 400 -500 °C was used[2].

For the SEM (section 6.3.2) and TEM images (section 6.3.3), the agglomeration that was observed could be attributed to the calcination temperature. This agglomeration also caused the diameters of the nanomaterials to increase. When the nanomaterials are calcined they agglomerate and form bigger particles[3].

The EDX of sample A1(Figure 6.4a) shows the presence of Ti, Na, and O. This means that there was a structural transformation. The EDX plots of the samples treated with NH_4OH (Figure 6.4 b-e) shows the presence of N but it is just overlapping with Ti and O. The EDX plots shows that even after the co-solvent approach, the structure of the titanate was the same as the one for sample A1.And this shows that NH_4OH had no influence in the structural transformation. Fe that was observed in the sample is from the autoclave since it is made from steel and Fe is one of the components of steel. So after treating the materials for 24 hours, there was black soot from the autoclave observed in the sample and it consisted of Fe.

The BET results shows that the surface areas of the materials decreased, and this decrease is attributed to the calcination temperature. When the material is exposed to heat, the particle size increases and the larger the particle size the smaller the surface area[2].

6.5 Conclusion

The calcined materials were found to be amorphous, there were no peaks that could be assigned to any structure of titania and this could be due to the low calcination temperature. Previous studies have shown that the crystallinity increases with the calcination temperature. The surface areas decreased because of the larger particle size. When the materials are calcined, they agglomerate and then forms larger particles and that result in the increase in diameters of the nanomaterials.

6.6 References

1. Sikhwivhilu, L.M., Mpelane, S.,Moloto, N. and Sinha Ray, S. **Hydrothermal synthesis of TiO_2 nanotubes: microwave heating versus conventional heating.**

2. Wong, C.L., Tan, Y.N., and Mohammed, A.R. (2011). **A review on the formation of titania nanotube photocatalyst by hydrothermal method**. Journal of Environmental Management, **92**, 1669-1680.

3. Sikhwivhilu, L.M, Sinha Ray, S, and Coville, N.J.,(2009).**Influence of bases on hydrothermal synthesis of titanate nanostructures**. Applied Physics A Materials science and processing, **94**, 963-973.

CHAPTER 7

The effect of calcination on the TiO_2 nanomaterials (KOH/ NaOH mole ratio)

7.1 Introduction

This chapter investigates the effect of calcination on TiO_2 nanomaterials that were treated with different mole ratios of KOH and NaOH. Section 7.2 outlines how the three samples (B1 to B3) were calcined and the various characterization techniques that were used. The results are given in the next section. Sections 7.3.1, 7.3.2, 7.3.3, 7.3.4 and 7.3.5 describe the XRD patterns, SEM images, TEM images, EDX plots and BET data. Lastly, sections 7.4, 7.5 and 7.6 give the discussion, conclusion and references.

7.2 Experimental

7.2.1 Calcination of TiO_2 nanomaterials

The nanomaterials that were calcined are given in chapter 5, Table 5.1 (samples B1 to B3). TiO_2 (P-25 Degussa) was reacted with different mole ratios of KOH and NaOH. The procedure that was outlined in chapter 6, section 6.2.1 was followed. After calcination, the samples were then named calcined B1, calcined B2 and calcined B3

7.2.2 Characterization of TiO_2 nanomaterials

The procedure that was outlined in chapter 6, section 6.2.2 was followed.

7.3 Results

The results obtained by five characterization techniques are given.

7.3.1 XRD patterns

The XRD patterns of the TiO_2 nanomaterials are shown in Figure 7.1. Calcined B1 shows sharp peaks at $2\theta = 25°$ and 27° and correspond respectively to anatase and rutile [1]. Calcined B2 show very small peaks. Samples B2 and B3 show no crystallinity and no diffraction peaks that can be assigned to any titania polymorphs. Instead these two samples have broad peaks.

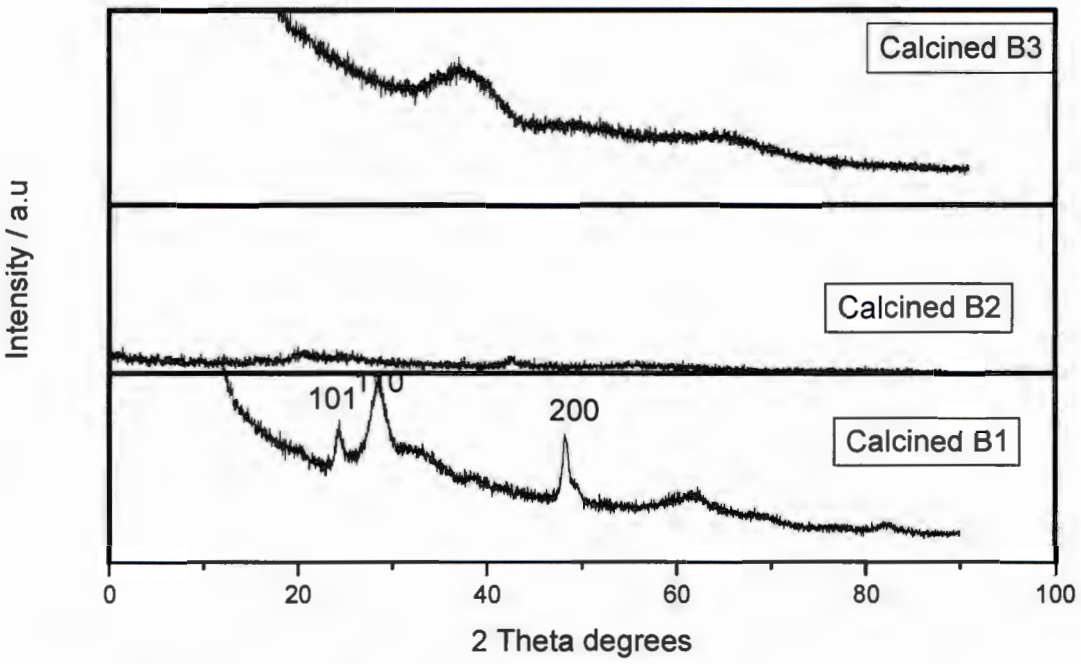

Figure 7.1: Indexed XRD patterns of the calcined samples [2,3]

7.3.2 SEM images

The SEM images are shown in Figure 7.2 (a-c). Figure 7.2 a is the SEM image of calcined B1, after calcination the quantity of nanotubes and nanorods increased. The SEM image of calcined B2 (Figure 7.2 b) shows the increase of nanobelts and nanowires. Lastly the calcined B3 shows the presence of clustered spherical aggregates. All these three samples are very agglomerated.

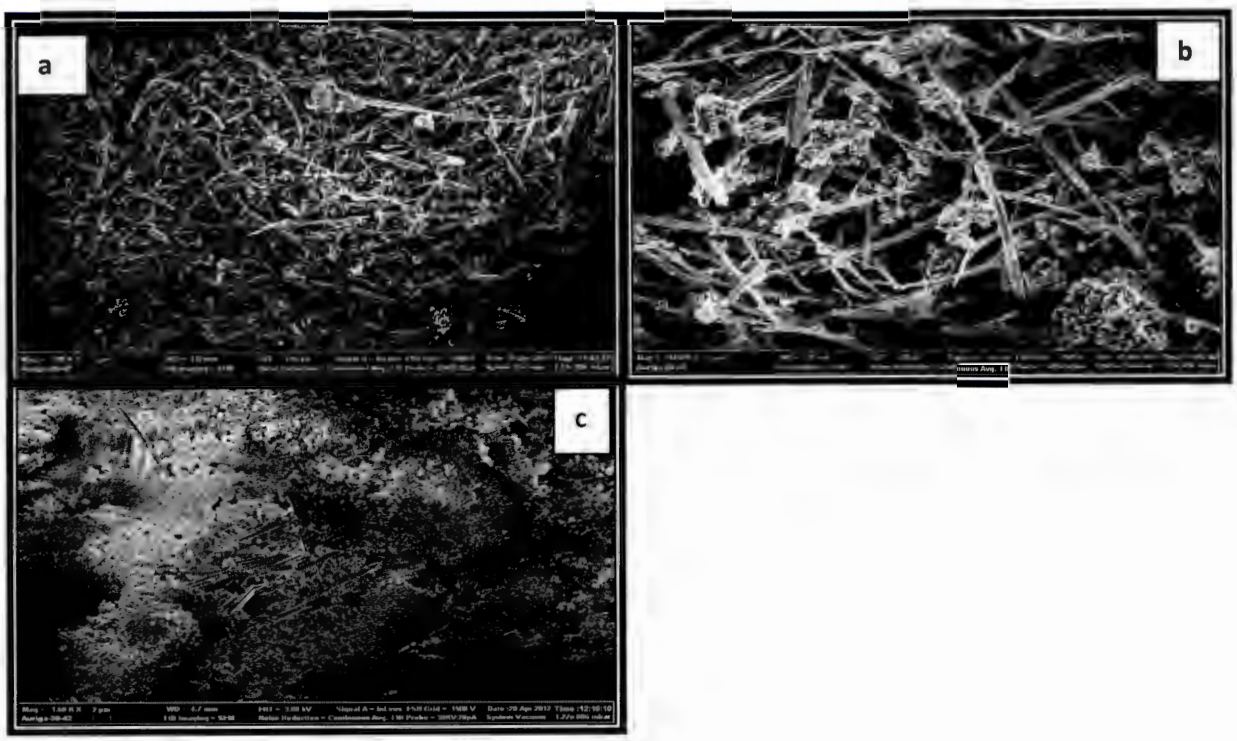

Figure 7.2:SEM images of (a) calcined B1 (b) calcined B2 and (c) calcined B3

7.3.3 TEM images

The TEM images of the nanomaterials are shown in Figure 7.3 (a-c). The calcined B1 (Figure 7.3 a) shows the presence of nanotubes and a very small proportion of nanorods, with an average diameter of 8 - 69 nm. The nanotubes are open-ended and single-walled. Figure 7.3 b represents the image of calcined B2, and it shows the presence of nanobelts and nanowires that are bundled together and have an average diameter of 10 – 143 nm. Calcined B3 (Figure 7.3 c) shows the presence of clustered spherical aggregates with an average diameter of 21 – 107 nm.

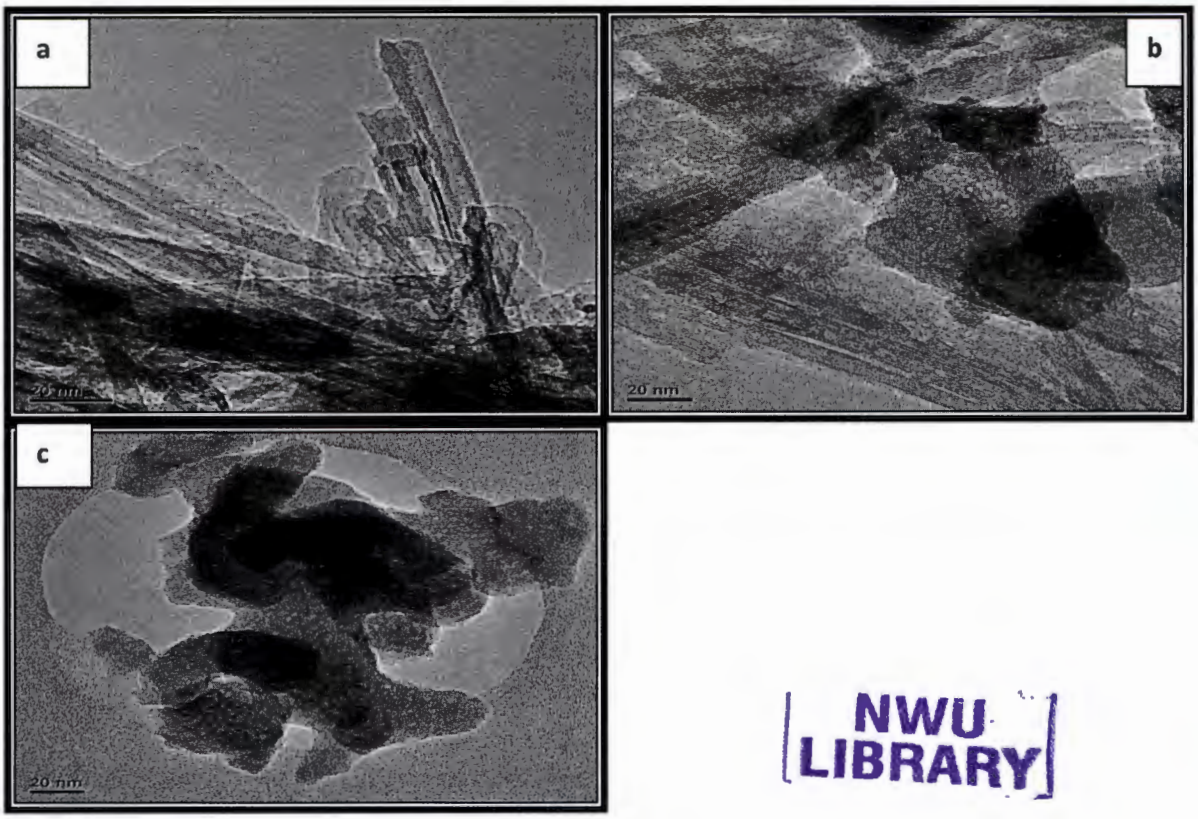

Figure 7.3: TEM images of (a) calcined B1 (b) calcined B2 and (c) calcined B3

7.3.4 EDX analysis

EDX analysis was done to determine the chemical composition of the materials. The plots are shown in Figure 7.4 (a-c). For all the samples, there is Na, K, Ti and Oxygen present. There are also small amounts of Al and Fe that are observed.

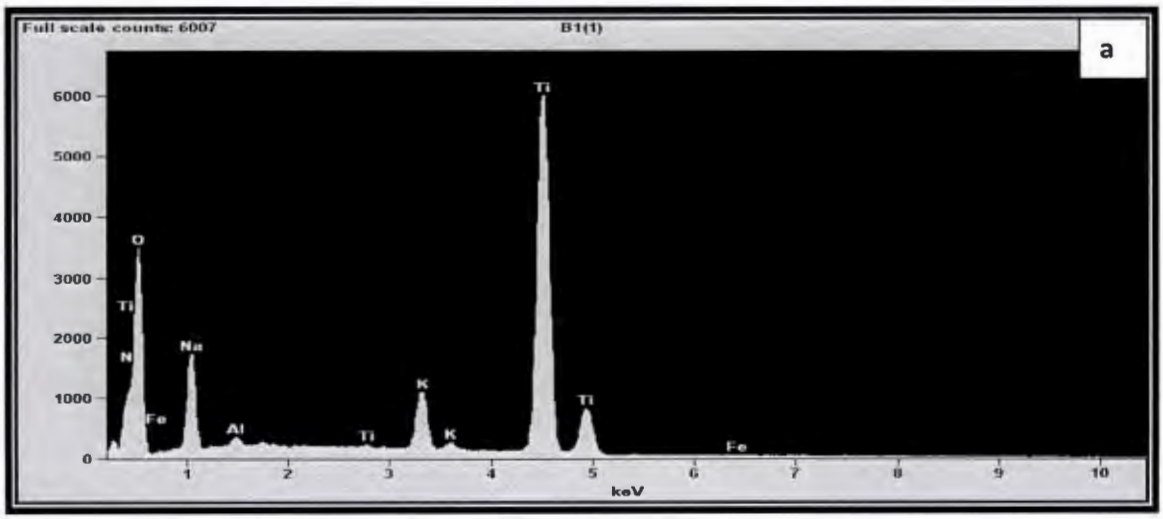

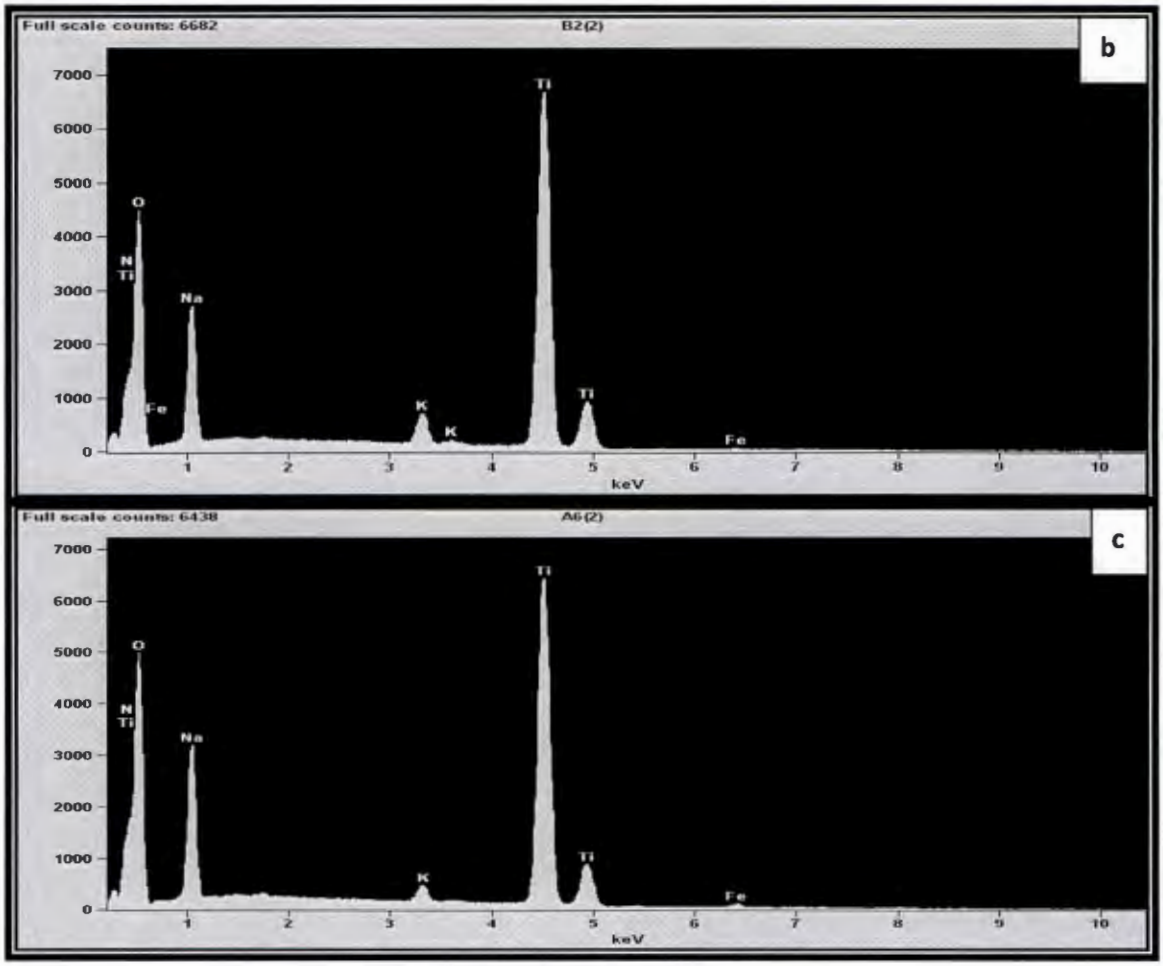

Figure 7.4 : EDX analysis of the calcined materials

7.3.5 BET results

The surface areas of the samples were determined by the BET method, and the results are tabulated in Table 7.1. For all the samples, the surface areas decreased.

Table 7.1 BET surface areas

Sample	**Surface area (m^2 / g)**
Calcined B1	95.5787
Calcined B2	60.8703
Calcined B3	26.4945

7.4 Discussion

The XRD patterns for the calcined B1 show peaks. This is because anatase and rutile are present in the sample. For the calcined B2 and B3, there were no peaks that could be assigned to any of the titania polymorphs. Instead these samples have broad peaks and they can be attributed to the presence of the titanate structure. All these three samples have a titanate structure because there is a structural transformation. For the SEM images, the increase in the amount of nanotubes, nanorods, nanowires and nanobelts is due to the calcination temperature. Although the used calcination temperature was low, it somehow managed to influence the morphology of these samples. This is because the calcination temperature is known to influence the morphology transformation of the samples. The agglomeration is also due to the calcination, because when the materials are heated they form bigger particles [4]. The TEM images show that the diameter of the materials have increased, and this is because of the increase in particle size. The EDX plots shows the presence of Na, K, Ti and Oxygen. This is not suprising since NaOH, KOH and TiO_2 were used in this experiment. Fe that was observed is from an autoclave, and the Al is from the Al stubs that were used for this (EDX) analysis. BET results show the decrease in the surface areas of the samples, and this is because of the increase in particle size. When the materials are heated they increase in size and the surface area decreases.

7.5 Conclusion

The nanomaterials were successfully calcined at 300°C for 4 hours. The calcination temperature played a huge role on the morphology of the materials, but it did not have an effect on the crystallinity. It was found that the amount of nanotubes, nanorods, nanowires and nanobelts increased after calcination.The surface areas decreased because of the increase in particle size, previous studies have shown that when the materials are heated they increase in size, therefore the surface area decreased. TEM results confirmed the increase in diameter size. EDX confirmed the presence of K, Na and Ti, and we can deduce that the materials consists of a titanate structure composed of K and Na.

7.6 References

1. Ohno, T., Sarukawa, K., Tokieda, K. And Matsumura, M. (2001). **Morphology of a TiO_2 Photocatalyst (Degussa, P-25) consisting of Anatase and Rutile Crystalline Phases.** Journal of Catalysis, **203**, 82-86.

2. Wang, X., Liu, G., Wang, L., Pan, J., Lu, G.Q and Cheng, H.-M. (2011). **TiO_2 films with oriented anatase {001} facets and their photoelectrochemical behavior as CdS nanoparticle sensitized photoanodes.** J. Mater. Chem., **21**, 869-873.

3. Watson, S., Beydoun, D., Scott, J. and Amal, R. (2004). **Preparation of nanosized crystalline TiO_2 particles at low temperature for photocatalysis**. Journal of Nanoparticle Research, **6**, 193-207.
4. Wong, C.L., Tan, Y.N., and Mohammed, A.R. (2011). **A review on the formation of titania nanotube photocatalyst by hydrothermal method**. Journal of Environmental Management, **92**, 1669-1680.

CHAPTER 8

The effect of loading Au on the TiO_2 nanomaterials

8.1 Introduction

This chapter considers the loading of Au on a TiO_2 support. Section 8.2.1 describes how Au was loaded onto the TiO_2 support. Section 8.2.2 describes the characterization of the Au / TiO_2 nanocomposites by XRD, TEM, EDX and BET. Sections 8.3 and 8.4 give respectively the results and discussion. Finally, sections 8.5 and 8.6 give the conclusions and references.

8.2. Experimental

8.2.1 Synthesis

Au loaded (5 % wt) samples were prepared by incipient wetness impregnation. Three samples were loaded, TiO_2 (P -25 Degussa), calcined B1 and calcined B2 (Chapter 7, section 7.2.1). 2g of the TiO_2 support was mixed with 0.2632 g of $HAuCl_4 . 3H_2O$ salt and then enough water to cover the mixture was added. The mixture was aged overnight. The mixture was subsequently centrifuged five times in order to remove the chloride ions and was calcined in a furnace at 300 °C for four hours. After four hours, the white colour of TiO_2 changed to purple and that indicated that the loading of Au was successful, and the Au^{3+} was reduced to Au^0 [1]. A summary of the synthesis is given in Table 8.1.

Table 8.1: Synthesis of Au / TiO_2 nanocomposites

TiO_2 support used	**Sample designation after loading**
TiO_2 (P-25 Degussa)	C1
Calcined B1	C2
Calcined B2	C3

8.2.2 Characterization

The loaded materials were then characterized according to the procedure given in chapter 4, section 4.2.2.

8.3 Results

8.3.1 XRD patterns

The XRD patterns of the loaded materials is shown in Figure 8.1. For Sample C1, the peaks are very sharp. There are peaks observed at 2θ = 25° and 27 ° and they can be assigned to anatase and rutile phases respectively. There are also peaks observed at 2θ = 38.06 °, 44.59 °, 62.93°, 75.31 ° and 82.98 ° and they correspond to (111), (200), (220), (311) and (222) Au diffraction peaks respectively. And the peak at 2θ = 38.06 ° was observed to be the overlap of Au with TiO_2 [2,3,4]. For Sample C2, there are also anatase and rutile phases observed at 2θ = 25° and 27 °. The Au diffraction lines were observed at 2θ = 38.37 °, 44.31°, and 62.84°. As for Sample C3, the anatase and rutile phases were observed at 2θ = 25° and 27° whereas the Au diffraction lines were observed at 2θ = 38.65 °, 44.23°, and 64.62° . But for Samples C2 and C3, the peaks especially the Au diffraction peaks are not sharp and crystalline like the ones for Sample C1.

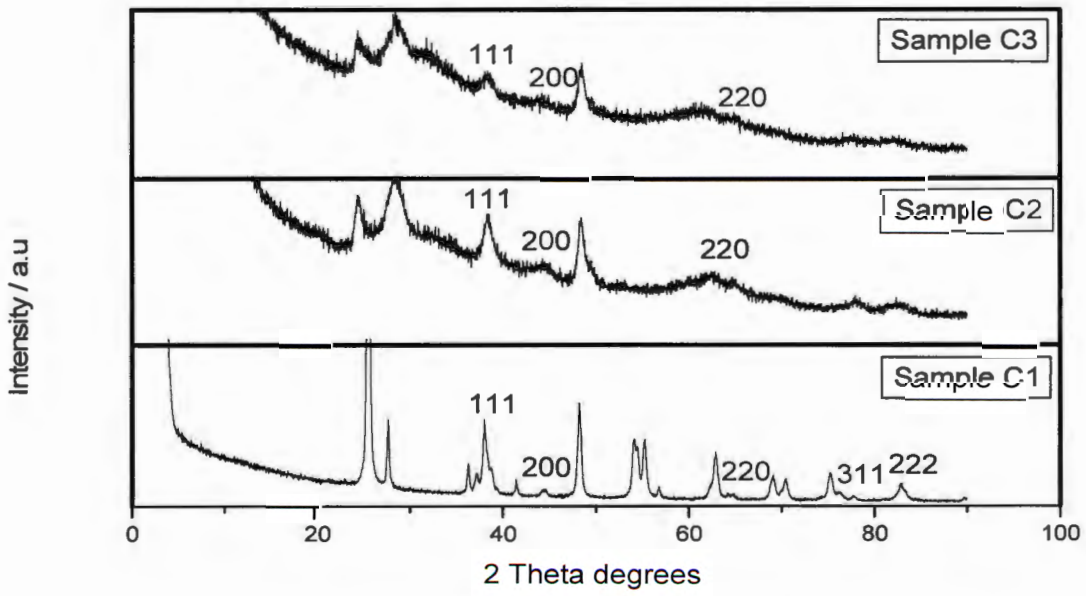

Figure 8.1: The indexed XRD patterns of the loaded materials [2,3,4]

8.3.2. TEM images

The TEM images of the loaded samples is shown in Figure 8.2 (a-c). For sample C1 (Figure 8.1), the Au particles were found to be well dispersed on the TiO_2. The Au particles were found to have an average diameter of 6 – 9 nm. Figures 8.2 b and 8.2 c show the TEM images of samples C2 and C3. The Au particles were found to be fairly distributed on the TiO_2 support, with average diameters of 15 – 19 nm and 7 – 20 nm respectively. For all the samples, Au particles were observed as dark spots on the surface of TiO_2 [5].

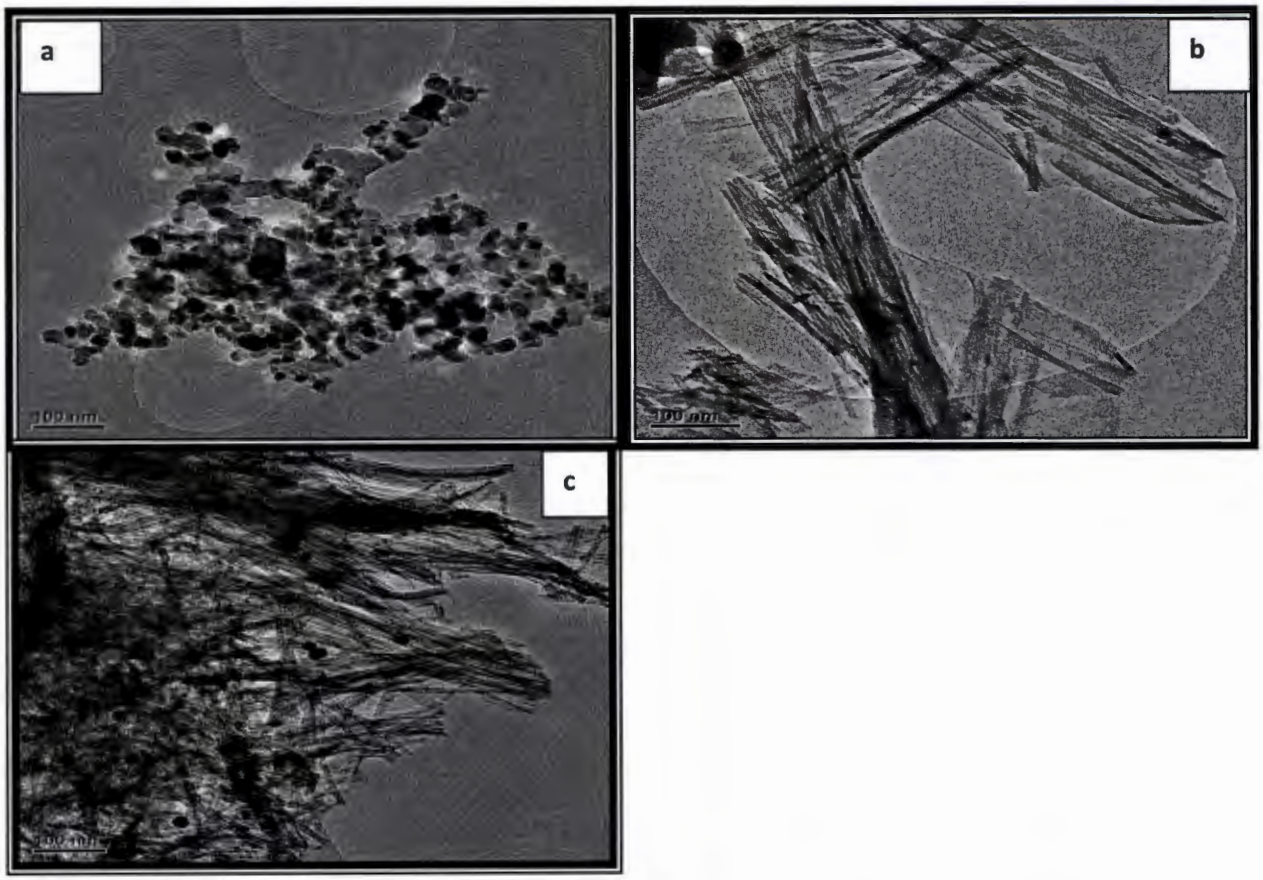

Figure 8.2 : TEM images of (a) Sample C1 (b) Sample C2 and (c) Sample C3

8.3.3 BET analysis

The BET surface areas are tabulated in Table 8.2. There was a slight increase in the surface areas of the loaded materials especially for the modified titania (samples C2 and C3). The surface area of sample C1 did not increase, in fact a slight decrease was observed.

Table 8.1 BET surface areas of the loaded materials

Sample name	Surface area (m^2 / g)
Sample C1	46.3755
Sample C2	105.3271
Sample C3	70.1533

8.3.4 EDX analysis

The chemical composition of the materials was examined by EDX, and the plots are shown in Figure 8.3. For Sample C1, the material is composed of Au, Ti and chloride ions. For Samples C2 and C3, the materials is composed of Au, Ti, K and Na. These two samples did not have chloride ions.

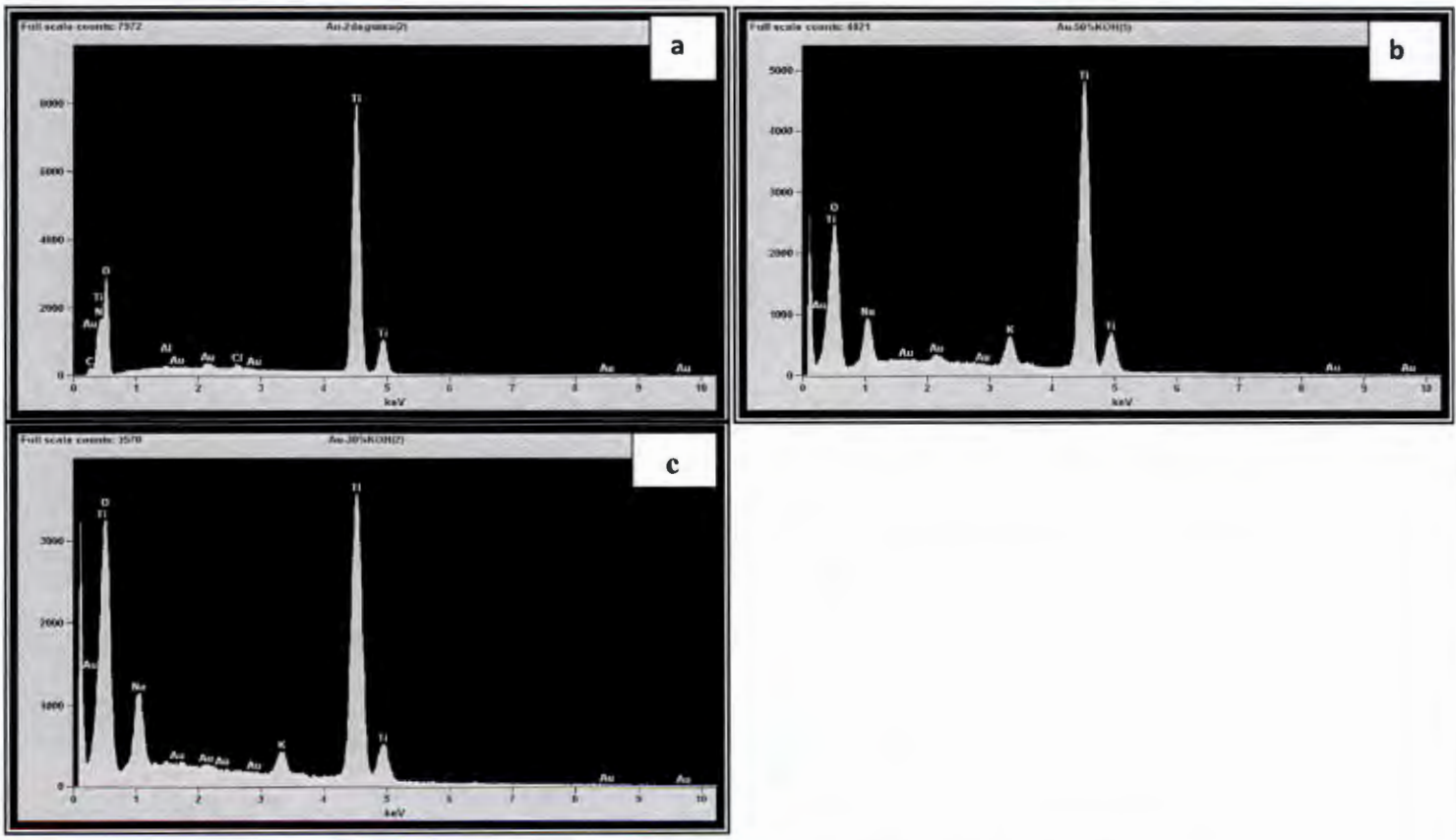

Figure 8.3 : EDX of the (a) Sample C1 (b) Sample C2 and (c) Sample C3

8.4 Discussion

The XRD patterns of C1, has sharp peaks because the material is very crystalline. Both samples C2 and C3 have a lower crystallinity than C1, this is because the supports that were used to synthesize these samples had low crystallinity. And this show that the loading of Au did not affect the crystallinity of these two samples. The difference in the XRD patterns of these samples could be due to the difference in the structure of the materials.

The TEM images show that the Au loaded on the spherical morphology becomes well dispersed than the ones on the tubular or rod-like morphology. And the average diameters of the Au particles on the spherical morphology were found to be less than the ones for the tubular and rod-like morphology. It has been shown that Au particles get well dispersed in the tubular morphology, depending on the method used and this usually happens when deposition-precipitation was used [6]. And in this study incipient wetness impregnation was used.

The increase in the surface areas of C2 and C3 can be attributed to the structural transformation. The slight decrease in the surface area of C1 could be due to the presence of chloride ions. This sample has a different structure than Cl. This is because the pH of TiO_2 P-25 Degussa was not adjusted with a base.

8.5 Conclusion

Au was successfully loaded on the TiO_2 by incipient wetness impregnation. The TEM results confirmed the loading and the Au particles was seen as dark contrasts on the TiO_2 . EDX also confirmed the presence of Au. Au particles were found to be well dispersed on the spherical morphology than on the tubular morphology, and this could be due to the method used. Incipient wetness impregnation method used here gave the best results when the support had a spherical morphology because it yielded small Au particles unlike tubular morphology. The surface areas of samples C2 and C3 increased due to the structural transformation. Because the XRD patterns of C2 and C3 differs with the ones for C2, it is therefore acceptable to say that their chemical structures also differs.

8.6 References

1. Li, W.-C., Comotti, M. And Schüth, F. (2006). **Highly reproducible synthesis of active Au / TiO_2 catalysts for CO oxidation by deposition-precipitation or impregnation.** Journal of Catalysis, **237** (1), 190-196.

2. Sun, X., Dong, S. and Wang, E. (2004). **Large-scale synthesis of micrometer- scale single-crystalline Au plates of nanometer thickness by a wet-chemical route**. Angew. Chem. Int.Ed, **43**, 6360-6363.

3. Jiao, J., Zhang, H., Yu, Li, Wang, X. And Wang, R. (2012). **Decorating multi-walled carbon nanotubes with Au nanoparticles by amphiphilic ionic liquids assembly.** Colloids and Surfaces A : Physicochemical and Engineering Aspects, **408**, 1-7.

4. Tang,W., Deng, L., Xu, K. and Lu, J. (2007). **X-ray diffraction measurement of residual stress and crystal orientation in Au / NiCr / Ta films prepared by plating.** Surface and Coating Technology, **201**, 5944 – 5947.

5. Haruta M. (1997). **Size- and support- dependency in the catalysis of gold**. Catalysis Today, **36**, 153- 166.

6. Méndez - Cruz, M., Ramírez – Solis, J. and Zanella, R. (2011). **CO oxidation on gold nanoparticles supported over titanium oxide nanotubes.** Catalysis Today, **166,**172 – 179.

CHAPTER 9

GENERAL CONCLUSIONS AND RECOMMENDATIONS

9.1 GENERAL CONCLUSIONS

Treatment of TiO_2 (P–25 Degussa) with 18 M NaOH yielded nanomaterials with spherical shape. However when the co–solvent approach was introduced whereby NH_4OH was used together with NaOH , the morphology still remained spherical. It was observed that NH_4OH did not alter the morphology and the structure of the nanomaterials. It was also observed that the nanomaterials treated by 18 M NaOH has a decreased diameter, and the structure of the material has been transformed. The nanomaterials prepared by the co-solvent approach showed an increase in diameters, and this is due to the formation of clusters.

When TiO_2 was further treated with KOH and NaOH, the morphology was transformed. The morphological transformation depended on the addition of KOH. When the amount of KOH was decreased, the morphology transformation decreased.The variations in the concentration of KOH led to different morphologies such as nanowires and nanobelts. The calcination temperature of 300 °C did not give good crystallinity. These nanomaterials experienced both structural and morphological transformations.

Au was loaded on the TiO_2 nanomaterials by incipient wetness impregnation method. TEM confirmed the presence of Au particles and they were seen as dark contrasts on the TiO_2 support. The presence of Au was further confirmed by EDX analysis.

9.2 RECOMMENDATIONS

The use of 10 M NaOH and 18 M KOH should be considered for future work to have a better understanding of its effect on the morphological transformations of TiO_2 (P25 Degussa). Loading Au / TiO_2 using deposition / precipitation method to compare the results with those obtained from incipient wetness method.

After synthesizing these nanomaterials, they will be incorporated in the membranes and they will be used to try to solve the problem of membrane fouling in membrane technology.